

Deanship of Graduate Studies

Al-Quds University



Physical Interactions between Digitonin and 1-Stearoyl-
2-oleoyl-*sn*-glycero-3-phosphocholine (SOPC) Using
Spectroscopic Techniques

Ibrahim Ghaze Mosa Hawwarin

M.Sc. Thesis

Jerusalem – Palestine

1439 / 2017

Physical Interactions between Digitonin and 1-Stearoyl-
2-oleoyl-*sn*-glycero-3-phosphocholine (SOPC) Using
Spectroscopic Techniques

Prepared by:

Ibrahim Ghaze Mosa Hawwarin

B.Sc : Physics science,AL-Quds University, Palestine.

Supervisor: Prof. Musa Abu Tair

Co- Supervisor: Prof. Hasan dweik

“A thesis submitted in partial fulfillment of requirement for the degree of
Master of Science from the department of Physics, Faculty of Science
and Technology, AL-Quds University.”

Jerusalem – Palestine

1439 / 2017

Deanship of Graduate Studies

Al – Quds University



Thesis Approval

Physical Interactions between Digitonin and 1-Stearoyl-2-oleoyl-*sn*-glycero-3-phosphocholine (SOPC) Using Spectroscopic Techniques

Prepared by: Ibrahim Ghaze Mosa Hawwarin

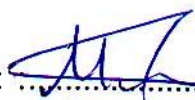
Registration No: 21213085

Supervisors: Prof. Musa Abu Tair

Co- Supervisor: Prof. Hasan dweik

Master thesis submitted and accepted, date 9 / 12 / 2017

The name and signature of the examining committee member are as follows:

1- Head of the committee: Prof. Musa Abu Tair	Signature: 
2. Internal Examiner: Dr. Husain Samamra	Signature: 
3. External Examiner: Dr. Lelia Mashal	Signature: 

Jerusalem – Palestine

1439/2017

Dedication

I dedicate this thesis to my family, especially, to my father and mother for their patience and understanding- to Dr. Sawsan Abu Sharkh and Dr. Saqer darwish for opening my eyes to the world.

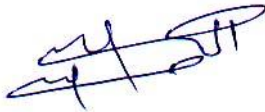
I also dedicate this work to many special friends in my life who always supported me and gave me the identity for being who I am. Special dedications go to my that teachers, I will always appreciate every nice and encouraging word have been said to me by my teachers for my entire life.

Ibrahim Ghaze Hawwarin

Declaration

I certify that this thesis submitted for the degree of master, is the result of my own research, except where otherwise acknowledged, and that this study has not been submitted for a higher degree or institution.

Signed:



Ibrahim Ghaze Hawwarin

Date: 9 / 12 /2017

Acknowledgements

I would like to take this opportunity to thank all those people who have contributed to this study and helped me complete this thesis.

Firstly I wish to thank my supervisor Dr. Musa Abu Tair for his support, encouragement and for providing me this opportunity to acquire the knowledge and expertise in the field of research. Thanks and appreciation to my committee Dr. Lelia Mashal (external examiner) and Dr. Husain Samamra (internal examiner).

Great thanks to every technician in Al-Quds University who helped me in my experimental work. Thanks to Mr. Waleed Keshi, Ms. Mariam Faroun and Ms. Leena Qra'a.

My thanks extend to my family, friends, who stood beside me and encouraged me constantly.

Finally, I wish to express my gratitude to the Almighty Allah for providing the grant to make this thesis possible.

Ibrahim Ghaze Hawwarin

Abstract

Digitonin is an amphiphilic steroidal saponin, a class of natural products that can bind to cholesterol and lyse cells. Despite the known cell membrane lysis activity, it remains unclear how it interacts with cell membranes. In the present work, the interaction mechanism between digitonin and 1-Stearoyl-2-oleoyl-*sn*-glycero-3-phosphocholine (SOPC) has quantitatively been investigated using a combination of physical techniques. Ultraviolet-Visible (UV-VIS) absorption spectrophotometry, Fluorescence absorption spectrophotometry and FT-IR spectroscopy, The values of the binding constants calculated at 293K are ($5.324 \times 10^3 M^{-1}$, $5.191 \times 10^3 M^{-1}$). The Stern-Volmer quenching constant values were found to be $1.05 \times 10^3 Lmol^{-1}$.

In this test with large unilamellar vesicles of (SOPC) and of different concentrations of digitonin, The interaction of digitonin with (SOPC) was determined, FTIR spectroscopy in the mid infrared region with Fourier self deconvolution, second derivative, difference spectra, peak picking and curve fitting were used to determine the effect of digitonin on the lipid, From the FTIR absorbance spectra, it is found that the intensity of the absorption bands decreased with increasing the concentration of digitonin that was injected with (SOPC).

Table of content

Abstract.....	vii
List of tables:.....	x
List of figures:	xi
List of symbols:	xiii
List of abbreviations:.....	xv
Chapter one: Introduction.....	2
1.1.1 Membrane.....	2
1.1.2 Lipids.....	3
1.2 Digitonin	4
Chapter two: Theoretical Background.....	6
2.1 Fourier Transform Infrared (FT-IR) development.....	7
2.2 Electromagnetic (EM) radiation and the photon	8
2.3 Wave propagation and absorption.....	10
2.4.1 Normal modes of vibration.....	12
2.4.2 Quantum mechanical treatment of vibrations.....	15
2.5 FT-IR spectroscopy	17
2.5.1. Infrared Spectroscopy.....	17
2.5.1.1 IR-Region	17
2.5.1.2 IR spectrum presentation	18
2.5.1.3 Principle of IR absorption	18
2.5.2 Theory of FT-IR spectroscopy.....	19
2.5.3. The sample analysis process by FT-IR spectrometer.....	21
2.6 Ultraviolet-Visible (UV-VIS) Spectrophotometer.....	22
2.7 Fluorescence Spectrophotometer.....	23
2. 8 Quenching.....	25
Chapter three: Experimental Part.....	26
3.1 Samples preparations.....	27
3.1.1 preparation of SOPC stock solution.....	27
3.1.2 Preparation of digitonin stock solution.....	27
3.1.3 Preparation of SOPC- digitonin solutions.....	27
3.1.4 Thin film preparation.....	26
3.2 Instruments.....	28
3.2.1 Fluorespectrometer (NanoDrop 3300).....	28
3.2.2 UV-VIS spectrophotometer (NanoDrop ND-1000).....	29
3.2.3 Fourier Transform Infrared spectroscopy (FT-IR)	29
3.3 Experimental procedure.....	30
3.3.1 Fluorospectrophotometer procedure	30
3.3.2 UV-VIS spectrometer (ND-1000).....	30
3.3.3 Fourier Transform Infrared (FT-IR) spectroscopy	31

Chapter four: Results and Discussion.....	33
4.1 UV-absorption spectroscopy	34
4.1.1 Determination of binding constant (K) by UV absorption spectroscopy	35
4.2 Fluorescence spectroscopy	36
4.2.1 Determination of Stern-Volmer quenching constants (K_{sv}) and the quenching rate constant (K_q)	37
4.2.2 Determination of the binding constant (K) by fluorescence spectroscopy	38
4.3 Fourier Transform Infrared (FTIR) spectroscopy.....	39
4.3.1 Peak positions.....	40
Chapter five: conclusions and future work.....	46
5.1 Conclusions	47
5.2 future work.....	47

List of tables.

Table 2.1: Molecule degrees of freedom.

Table 2.2: Typical bond stretching and angle-bending group vibrations.

Table 4.1: The bands were tentatively identified on the basis of reference standards and published FTIR spectra in relation to specific molecular groups.

Table 4.2: Bands assignment in the absorbance spectra of SOPC with different digitonin concentrations .

List of Figures:

Figure No.	Figure caption	page
Figure 1.1	Membrane component.	3
Figure 1.2	Various lipids found within a cell. SOPC, POPC, and DOPC are phospholipids.	4
Figure 1.3	Chemical structure of digitonin.	4
Figure 2.1	The electromagnetic spectrum in different units .	9
Figure 2.2	Conceptual division of the mid IR spectra of Hexanol into functional and fingerprint regions.	13
Figure 2.3	potential energy of a diatomic molecule as a function of atomic displacement (inter-nuclear separation) during vibration. The Morse potential (blue) and harmonic oscillator potential (green) .	16
Figure 2.4	Regions of IR spectrum .	18
Figure 2.5	Schematic of a Michelson interferometer: The initial IR beam is split by the beamsplitter. The two split beams move different distances and have different phase delays when recombined, hence causing an interference pattern (an interferogram).	20
Figure 2.6	FT-IR spectrometer layout and basic components .	22
Figure 2.7	Relative energies of orbitals most commonly involved in electronic spectroscopy of organic molecules .	23
Figure 2.8	The Jablonski diagram of fluorophore excitation .	24
Figure 3.1	Excitation LEDs.	29
Figure 4.1	UV absorbance spectra of SOPC-digitonin complexes at different digitonin concentrations (a: 0.0mM, b: 0.1mM, c: 0.2mM, d: 0.3mM, e: 0.4mM, f:0.5mM, and g:0.6mM).	34
Figure 4.2	the plot of $\frac{1}{A-A_0}$ VS $\frac{1}{L}$ for SOPC with different concentrations of digitonin.	35

Figure 4.3	The fluorescence emission spectra of SOPC with various concentrations of digitonin (0.1, 0.2, 0.3, 0.4, 0.5, and 0.6 mM).	36
Figure 4.4	The plots of $\frac{F_0}{F}$ vs [L] for SOPC-digitonin complexes.	37
Figure 4.5	The plot of $\frac{1}{F_0-F}$ vs $\frac{1}{L}$ for SOPC-digitonin.	38
Figure 4.6	the hydrophobic region (CH ₂ stretching), the interfacial region (C=O stretching) and the polar region (P-O ²⁻ stretching) are depicted in the.	39
Figure 4.7	The second derivative of the FTIR spectrum for SOPC free in The three regions.	40
Figure 4.8	The FTIR spectra of SOPC-digitonin thin films with concentrations (0.1, 0.2, 0.3, 0.4, 0.5 and 0.6 mM) .	41
Figure 4.9	The second derivative of the FTIR spectrum for SOPC free in CH ₂ stretching vibration.	41
Figure 4.10	The FTIR spectra of free SOPC .	42
Figure 4.11	The FTIR spectra of SOPC-digitonin thin films with concentrations (0.1, 0.2, 0.3, 0.4, 0.5 and 0.6 mM) .	42
Figure 4.12	The second derivative of the FTIR spectrum for SOPC free in C=O stretching and P-O ²⁻ stretching vibration .	43
Figure 4.13	The FTIR spectra of free SOPC in C=O stretching and P-O ²⁻ stretching vibration.	44
Figure 4.14	The FTIR spectra of SOPC-digitonin in C=O stretching and P-O ²⁻ stretching vibration thin films with concentrations (0.1, 0.2, 0.3, 0.4, 0.5 and 0.6 mM) .	44

List of symbols:

symbol	description
Δ	Un-saturation site
K	Binding constant
λ	Wavelength
h	Planck's constant
N	Frequency
E_{total}	Total energy
E_{ele}	Electronic energy
E_{vib}	Vibrational energy
E_{rot}	Rotational energy
m_A, m_B	Mass of particles A,B
Δx	Displacement of the spheres along the x-axis from equilibrium position
F_x	Restoring force acts on the spheres
F	The spring or force constant
V	The potential energy
T	The kinetic energy of the oscillating motion
μ	The reduced mass
$\Delta x'$	Velocity
Ω	Circular frequency of the harmonic vibration
C	Speed of light
ν	Circular frequency in wave-numbers
E_ν	The potential energy for harmonic oscillator approximation
V	Vibrational level
A	Constant for a particular molecule.
D_{eq}	The dissociation energy.
ω_e	Oscillating frequency
$\hat{\omega}_e$	Oscillation frequency in wave number
X_e	The an-harmonic constant
R	Inter-nuclear separation
$E_0(\nu)$	The maximum amplitude of the beam at $z=0$
I_0	The radiant power incident on the sample
$I(z_1, z_2, \nu) d\nu$	The intensity after recombination of the beams for the fixed spectral range $d\nu$
$S(\nu)$	The spectrum
A_0	The initial absorption of protein at 280 nm in the absence of ligand

A_{∞}	The final absorption of the ligated protein
A	The recorded absorption at different Testosterone concentrations (L).
S ₀	The ground singlet electronic state
S ₁ and S ₂	The successively higher energy excited singlet electronic states
T ₁	The lowest energy triplet state
$h\nu_{EM}$	Energy of photon emitted
$h\nu_{EX}$	The excitation photon energy
K	The Stern-Volmer quenching constant
k_q	The bimolecular quenching constant
T	The unquenched lifetime
[Q]	The quencher concentration.
F ₀	Fluorescence intensity without quencher
F	Fluorescence intensity with quencher
K _{sv}	The Stern-Volmer quenching constant
L	The quencher concentration
B	The path length
A	The absorptivity

List of abbreviations:

abbreviation	Abbreviation representation
SOPC	1-Stearoyl-2-oleoyl- <i>sn</i> -glycero-3-phosphocholine.
DOPC	1,2-Dioleoyl- <i>sn</i> -glycero-3-phosphocholine.
POPC	1-Palmitoyl-2-oleoyl- <i>sn</i> -glycero-3-phosphocholine.
pH	Power of hydrogen
UV-VIS	Ultraviolet –visible light
FT-IR	Fourier Transform Infra-red
CAT	Computer assisted tomography scanning
PET	Positron Emission Tomography
IR	Infra-red
FSD	Fourier self deconvolution
EM	Electromagnetic
Mid-IR	Middle infrared
T	Transmittance
A	Absorbance
C	Concentration
LED's	Light emitting diodes
Diff	Difference

Chapter One:
Introduction

Chapter one.

Introduction.

This research work is concerned with using spectroscopic techniques such as Fourier Transform Infrared Spectroscopy (FTIR), UV-Vis spectroscopy and Fluorescence spectroscopy to investigate the effect of digitonin on SOPC lipid.

The first spectroscopic technique that is used in this work was FTIR which is used in order to investigate the conformational changes structure of SOPC upon the addition of different concentrations of digitonin on it. Investigation of structural changes includes changes in peak positions and peak relative intensities .

UV-absorption spectroscopy is the second spectroscopic technique that is used to investigate the strength of interaction between SOPC with digitonin. The binding constant between SOPC and digitonin was determined.

Fluorescence spectroscopy was used to confirm the calculation of binding constants as an indication of the strength of interaction. The Stern-Volmer quenching constants for digitonin interaction with SOPC will also be calculated.

This thesis includes five chapters; The first chapter is an introduction. It shows the purpose and the importance of this work. It also gives information about each chapter in this thesis. chapter two will discuss the theoretical aspects to guide readers to the important ideas of this study. Chapter three includes details of the experimental, procedures, and instruments used. In chapter four the results obtained are presented and discussed. Final chapter contains the conclusions and future work.

1.1.1 :Membrane.

Biological membranes consist of lipids, proteins, and carbohydrates. Figure 1.1 shows the basic unit of the membrane which is the bilayer. Bilayer is formed by lipids organized in two layers with their polar headgroups along the two surfaces and their acyl chains forming the nonpolar domain in between. Integral membrane proteins are embedded in the lipid bilayers, which cannot be removed without disturbing the membrane.(Luckey 2008, Nelson 2004)

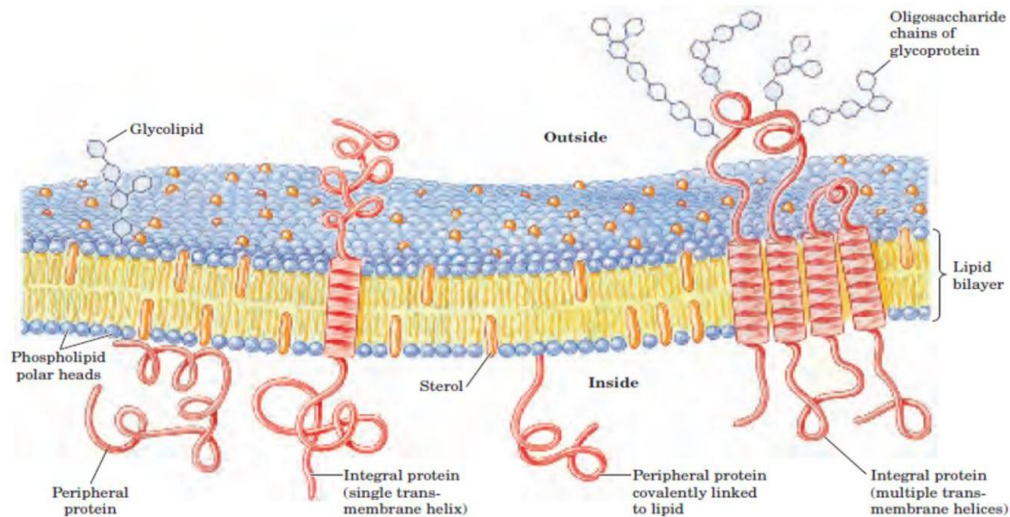


Figure 1.1 Membrane component.(Nelson 2004)

Membranes are responsible for the selective permeability of cell envelopes that enables cells to take up many nutrients and exclude most harmful agents. The permeability is determined by both lipid and protein component of membranes. Proteins in the membrane make channels and transporters for ions and hydrophilic substances (Hannun 2008).

Membrane is a very dynamic structure with constant activity on the surface as well as constant movements in the bilayer. The fluid nature of the membrane comes from the lateral movement. This movement enables interactions among proteins and between proteins and lipids to provide temporal associations that are important to membrane functions (Takai1979).

1.1.2 :Lipids.

Lipids found in biomembrane are divided into three main classes of lipids, which are glycerophospholipids (or phospholipids), sphingolipids, and sterols and linear isoprenoids. The backbone of membrane phospholipids is the isomer called sn-glycerol-3-phosphate. With fatty acyl chains in ester linkage on carbons 1 and 2, it becomes phosphatidic acid. The estrification of phosphatidic acid with another alcohol creates the following phospholipids: phosphatidylcholine (PC), phosphatidylethanolamine (PE) , phosphadidylserine (PS), phosphatidylglycerol (PG), and phosphatidylinositol (PI). These abbreviations are coupled with the abbreviated common names for acyl chains; for example, DOPC is 1,2-Dioleoyl-*sn*-glycero-3-phosphocholine, POPC is 1-Palmitoyl-2-oleoyl-*sn*-glycero-3-phosphocholine, and SOPC is 1-Stearoyl-2-oleoyl-*sn*-glycero-3-phosphocholine (Nelson 2004). Figure 1.2 shows the chemical structures of DOPC, POPC, and SOPC. The phosphate groups and headgroups are the polar portions, and the acyl chains are the nonpolar parts of these amphiphilic molecules.

The structure of the lipid used for this work are diagrammed in Figure 1.2. SOPC (1-stearoyl-2-oleoyl-*sn*-glycero-3-phosphatidylcholine) has two 18 carbon (Gomez-Fernandez 2007).

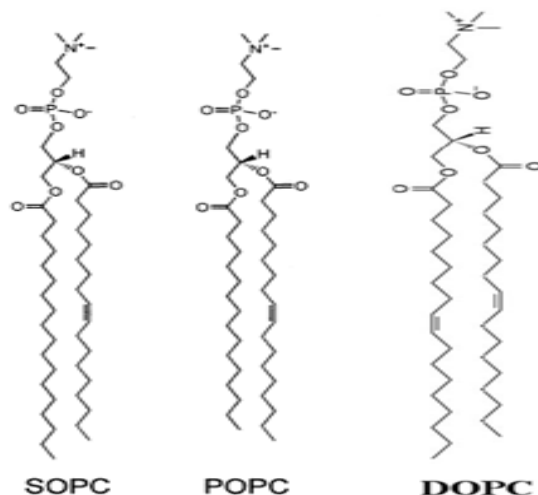


Figure 1.2 : Various lipids found within a cell. SOPC, POPC, and DOPC are phospholipids.

1.2: digitonin.

Saponins represent an important class of bioactive secondary metabolites produced mainly by plants which serve as natural defense compounds against herbivores and microbial infections (Keukens 1992). Saponins are present in many medicinal plants which have been used as anti-inflammatory, secretolytic, anti-fungal, anti-bacterial, cholesterol-lowering, anti-cancer drugs and as an adjuvant for vaccinations (Hostettmann 1995,). Chemically, saponins are either triterpenes or steroids (De Geyter 2012, Thakur 2011), which can carry one or several hydrophilic oligosaccharide chains connected to the aglycone via glycosidic or ester bonds (Thakur 2011). In plants, saponins are stored in the vacuole as inactive bidesmosides which carry at least two sugar chains. When a plant is wounded or infected, a glucosidase or esterase is released which cleaves one of the sugar chains producing the bioactive amphiphilic monodesmosides (Wink 2008). Figure 1.3 shows the chemical structures of digitonin.

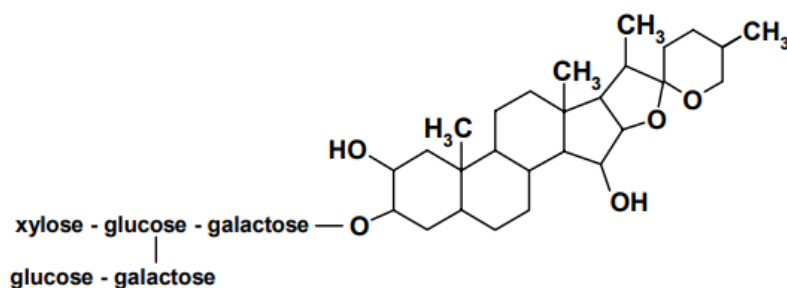


Figure 1.3: Chemical structure of digitonin.

Such an amphiphilic nature of many saponin derivatives results in a strong surface activity, which can be used to make cell membranes permeable to allow for the access of various small molecules to nuclei and intracellular organelles (Liu 1999). Higher concentrations of monodesmosidic saponins completely lyse cells, which can easily be demonstrated using red blood cells. Digitonin, one of the steroidal saponins found in *Digitalis* species, has been widely used for the cell membrane permeabilization. Although other commonly used agents, such as Triton, glycerol, and toluene, interact non-specifically with cell membranes (Fiskum 1980), accumulating evidence suggests that digitonin specifically interacts with membrane sterols (Akiyama 1980, Yu 1986).

The increase in the permeability of ions (Murphy 1980), metabolites (Murphy 1980, Zuurendonk 1974) and enzymes (Zuurendonk 1974) across cell membranes can be attributed to the decrease in the packing of hydrocarbon chains caused by the removal of sterols, which fill defects and free voids in the hydrophobic membrane core. The higher selectivity of digitonin activity toward cell membranes than organelles (Keukens 1992, Stearns 1982) actually seems plausible if one considers the fact that cholesterol and other 3-hydroxysterols are present at high molar ratios in cell membranes (Fiskum 1980).

Chapter Two:
Theoretical Background

Chapter two

This chapter will cover theoretical aspects of this work, the first two sections will include a short historical background on the development of FT-IR spectroscopy and electromagnetic spectrum, next section will cover briefly molecular vibrations, the following three sections discuss the spectroscopic approaches used in this work; FT-IR, UV-VIS, and fluorescence spectrophotometers.

2.1 Fourier Transform Infrared (FT-IR) development.

FT-IR spectroscopy has been used to study the secondary structure composition, structural dynamics, conformational changes (effects of ligand binding, temperature, pH and pressure), structural stability and aggregation of proteins. Such information can be deduced from the spectral parameters: band position, band width and absorption; this standing due to the sensitivity and stability of spectrophotometers; which are valuable tools for the investigation of protein structural changes during molecular interactions (Kong, J et al. 2007). IR spectroscopy is one of the most common spectroscopic techniques used for structure determination in biological systems, due to high information content in an IR spectrum and its sensitivity to the chemical composition of molecules. (Uversky et al. 2007).

The discovery of infrared light can be dated back to the 19th century. Since then, scientists have established various ways to utilize infrared light. Sir William Herschel was the first to recognize the existence of infrared in 1800. In the late 1800s, Albert Michelson developed the interferometer for studying the speed of light. During 1882-1900 several investigations were made into the IR region. Because of the numerical complexities of the Fourier procedure, it was not until 1949 that Peter Fellgett calculated a spectrum from an interferogram. In 1964, the discovery of the fast Fourier transform (FTT) algorithm by James Cooley and John Tukey reduced the time for the computer calculation of the transform from hours to just few seconds and spectacular advances have been made in the instrumentation from single beam to double beam dispersive spectrometers (Derrick, M.R et al. 1999). As was reported by Lakowicz, 2006; a number of mathematical techniques, such as Fourier self deconvolution (FSD) and derivative, have been developed to study proteins, also number of tools such as fluoru-spectrophotometer became a widely used scientific tool in biophysics and material science after pioneering research of Kasha, Vavilov, Perrin, Weber, Stockes and Forster in 1951 (Iakowicz 2006).

2.2 Electromagnetic radiation and the photon.

Radiation can be described as an electromagnetic sine wave, comprising of both electric and magnetic field components. Electromagnetic interactions result from the exchange of photons as the electromagnetic field is quantised, in quantum mechanical terms. Electromagnetic radiation is classified according to the frequency of its wave in the electromagnetic spectrum (Flower 2011).

Spectroscopy is defined as the study the interaction of radiation with matter. Radiation is characterised by its energy, E . Radiation is emitted and absorbed in the tiny packets called photons. Photons can be described in two ways. Firstly, they can be said to hold particle properties, moving in straight lines at the speed of light. Photons have no detectable 'rest' mass, which enables them to travel at light speed with respect to all observers. Photons do, however, have both energy and momentum and the photon energy will be conserved unless emitted or absorbed by a charged particle. Einstein's equation ($E=MC^2$) cannot describe their energy however as they have no mass. Plank devised a constant to describe the relationship between photon energy and frequency (Stuart 2004).

The energy of the photon particle can be described mathematically (eq. 1) where h is Planck's constant (6.626×10^{-34} J.s) and ν is the frequency (Hz).

$$E= h \nu \dots\dots\dots(\text{eq. 1})$$

According to 'wave-particle duality' in quantum physics, it is natural for the photon to display either particle properties or wave properties, according to its circumstances. Waves have two important characteristics, frequency ν and wavelength λ related by the speed of light c in a vacuum (2.998×10^8 m/s)(Flower 2011) (eq.2).

$$\nu= c/\lambda \dots\dots\dots(\text{eq.2}).$$

Therefore radiation, characterised by its energy E , is linked to the frequency ν and wavelength λ of the radiation by the Planck relationship .

The energy of the electromagnetic wave is proportional to the frequency, or inversely proportional to the wavelength (eq. 3)

$$E= h\nu= hc/\lambda \dots\dots\dots(\text{eq. 3})$$

Where E is the energy, h is Planck's constant, ν is frequency, and λ is wavelength (Pavis et al 2008, Yadav 2005, Williams 1976, Ball 2001).

Vibrational spectroscopy in particular uses the reciprocal wavelength ($1/\lambda$) which is the number of wavelengths per unit distance, denoted as wavenumber (Flower 2011).

Vibration and rotation of atoms and molecules can be represented by discrete energy levels. A stream of particles, i.e. quanta, of energy interacts with matter by either absorption or emission. However, in order for interaction to occur, a quantum of energy must exactly fit between neighboring energy levels (Stuart 2004). For instance, given two neighboring atomic energy levels E_1 and E_2 , absorption occurs when frequency is given by:

$$\nu = (E_2 - E_1) / h \dots\dots\dots(\text{eq. 4})$$

The electromagnetic radiation spectrum ranges, in wavelength, from millions of kilometers to fractions of femtometers, and is conventionally divided in many regions, as illustrated in Figure 2.1. In terms of wavelength, the infrared region spans from 1mm to 750nm, and is divided into three sub-regions: near (i.e. 0.75-5 μm), mid (i.e. 5-30 μm) and far (i.e. 30-1000 μm) infrared. The near infrared region is closest to the visible spectrum, whereas the far infrared, as the name implies, is farthest (Hollas 2004).

Most of the discussion from here on will be concerned with the mid infrared region. Care must be taken when using these infrared sub-region definitions, since there is no international standard for these specifications, and authors often disagree on the subject (Turro 1991).

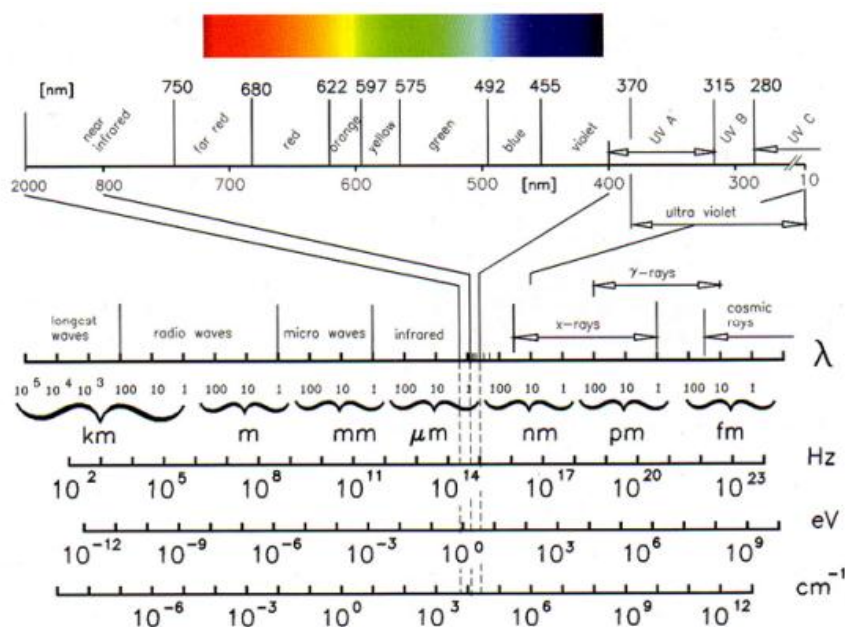


Figure 2.1: The electromagnetic spectrum in different units (Schmidt, 2005).

2.3 Wave propagation and absorption.

One way to make the connection between particle and wave descriptions of a photon is to visualise a propagating wave packet. The speed of a wave depends upon the medium in which it propagates. The propagation of an electromagnetic wave in a non-absorbing medium can be described mathematically as (eq. 5).

$$A(\varphi) = A_0(\varphi) e^{i(\omega t - \delta)} \dots\dots\dots(\text{eq. 5}) .$$

where A is the amplitude, ω is the angular frequency, t is the time, δ is the phase angle and φ is the polarisation angle (Flower 2011). The angular frequency is a measure of how fast an object is rotating about its axis and is expressed by the wavelength and refractive index n (Flower 2011). (eq. 6).

$$\omega = c/\lambda n \dots\dots\dots(\text{eq. 6}).$$

The refractive index must be modified to its complex form in the case for an absorbing medium (eq.7).

$$n^* = n + ik \dots\dots\dots(\text{eq. 7})$$

Here, the real part of the refractive index n is the ratio between c and the speed at which light travels in a material, known as the phase velocity v_p (eq. 8).

$$n = c/v_p \dots\dots\dots(\text{eq.8})$$

When infrared radiation passes through a material, or medium, some intensity is absorbed through interaction with the molecules, and some intensity passes through without interaction. For an absorbing medium, the absorption coefficient α is one of many ways to describe the absorption of electromagnetic waves. α can be expressed in terms of the imaginary part of the refractive index k and the wavelength of light (eq. 9). The imaginary part k indicates the amount of absorption loss when the wave propagates through the material (Flower 2011).

$$\alpha = 4\pi k/\lambda \dots\dots\dots(\text{eq. 9})$$

Based on eq. 5, the transmittance of radiation at intensity I emerging through a material is related to the intensity of incident radiation I_0 at the front face of the material, at a particular wavenumber (eq.10). The Beer Lambert Law results directly from this equation where λ (cm) is the path length of the wave within the absorbing medium (optical thickness) and ϵ is the molar absorption coefficient and c the concentration (mol dm^{-3}) of the absorbing material (eq.11) (Flower 2011).

$$I = I_0 e^{-\epsilon cl} \dots\dots\dots(\text{eq.10})$$

$$T = I / I_0 = 10^{-\epsilon cl} \dots\dots\dots(\text{eq.11})$$

The proportion of absorbed intensity of radiation over the total intensity that enters the material has a direct relation to the concentration of the material. Absorbance becomes linear with concentration (eq. 12) (Krishan 1975).

$$A = \log(I_0 / I) = \epsilon cl \dots\dots\dots(\text{eq.12})$$

Absorbance is the negative logarithm of the transmittance (T) (eq. 13).

$$A = \log(1/T) = -\log(T) = -\log(I/I_0) \dots\dots\dots(\text{eq.13})$$

In the Beer-Lambert law, the concentration of an unknown material can be found by using the absorbance at a single wavelength. An absorbance spectrum, however, is a distribution of absorbance intensities for radiation passing through a sample over a series of wavelengths. Absorption varies with wavelength as the absorption coefficient has a different value at each wavelength (Krishan 1975).

When an interferogram is Fourier transformed it results in an output of light intensity at the detector versus the optical frequency. This raw, single beam spectrum contains information about the whole instrument; the sample, the sources, the ambient air, the optical components as well as any possible contamination in the optical path. As only the information due to the sample itself is of interest, first a reference spectrum called the background must be acquired and used to remove unwanted information from the raw spectrum. The reference spectrum only contains information about the environment in the instrument and all reference spectra for FTIR spectrometers have the same general shape (Hollas 2004, Schulman 1977).

To obtain the absorbance spectrum of the sample, the value at each wavelength in the sample spectrum is divided against the corresponding value at the same wavelength in the reference spectrum and the negative logarithm is taken (eq. 14). (Krishan 1975).

$$A = -\log(\text{sample /reference}) \dots\dots\dots(\text{eq.14})$$

2.4.1 normal modes of vibration.

Fundamentally, the field of infrared absorption spectroscopy strides to determine the differences in energy caused by the absorption of infrared radiation when reflected or transmitted through a medium. In order for infrared absorption to occur, energy must cause a change in a molecule's electric dipole moment. This assertion is referred to as the *selection rule*. The selection rule implies that only heteronuclear diatomic or polyatomic molecules may show absorption in the infrared region.

Changes in the dipole moments of a polyatomic molecule can be considered in terms of molecular vibrations and rotations. These movements occur according to the Figure 2.2. The electromagnetic spectrum in different units (Schmidt, 2005).molecule's degrees of freedom. There are basically three types of degrees of freedom, translational, rotational and vibrational. The total number of a molecule's degrees of freedom is the sum of translational, rotational and vibrational degrees of freedom. For any molecule with N atoms, it follows that the total number of degrees of freedom it possesses is $3N$. A general rule of thumb is that, since larger molecules have more degrees of vibration, they generally have many more peaks of absorption than smaller molecules. In addition, bonds of atoms that are farther away in the periodic table shows stronger bands than the contrary because they have stronger dipole momentum (Stuart, 2004).

Each molecule produces a unique infrared absorption spectrum because of its particular bonds and structures. A mid infrared absorption spectrum of a molecule may be conceptually divided into two regions, namely the functional-group region and the fingerprint region. To illustrate this idea, Fig 2.2 shows the plot of the mid infrared spectrum of Hexanol, with the marked division between functional and fingerprint regions. As with the determination of near, mid and far infrared regions, there is currently no international standard or governing body to establish a set of specification to define these regions. The functional region is considered to have absorption bands due to molecular functional group bonds, whereas the fingerprint contains the response to the intrinsic skeletal vibrations, mostly unique to each molecule.

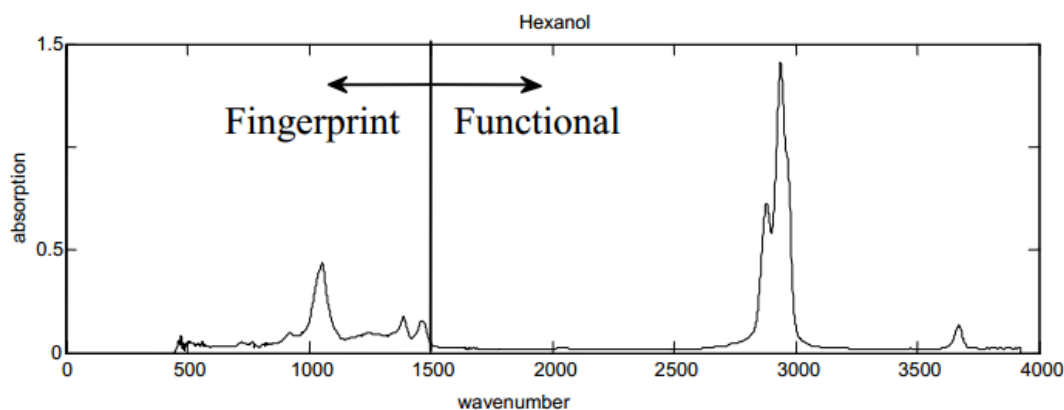


Fig 2.2: Conceptual division of the mid IR spectra of Hexanol into functional and fingerprint regions.

The division of the infrared spectrum into functional and fingerprint regions is important to analytical spectroscopy. The functional region typically offers more general information about a certain compound's chemical structure than the fingerprint region. By performing spectral analysis of the principal bands found in the functional region, we are generally able to correlate the sample to functional groups, which is particularly useful in the preliminary steps of molecular identification. On the other hand, infrared absorption in the fingerprint region of molecules that belong to the same functional group can be quite different. Peaks in the fingerprint region are very useful for classification, or in the last steps of molecular identification.

There are many factors that can make experimental infrared spectroscopy less than straightforward, and which can complicate a successful interpretation of the spectrum. When first observing infrared absorption profiles, one may easily realize that absorption bands aren't infinitely narrow. Broadening of bands can be attributed to many factors such as collision between molecules, finite lifetime of state transitions, time varying energy states or the Doppler effect (Stuart, 2004).

Experimentally, spectral absorption lines of molecules may vary tremendously because of solvents, temperature and other environmental factors in place. Different temperatures may cause fluctuation in the number of vibrational and rotational degrees of freedom. For instance, at low temperatures one can selectively freeze degrees of rotational freedom (Schmidt, 2005). Solvents may interact with the molecule, also causing a change in a molecules' absorption lines. Nonetheless, in most cases, the major absorption lines of a given molecule are still apparent regardless of the solvent used or temperature changes.

In addition, there are other complicating factors such as overtone, combination bands, Fermi resonance, coupling and vibration-rotation bands. Overtone bands are integer multiples of the fundamental frequency, which is proportional to wavenumber. A spectral measurement may show energy absorbed at a fundamental frequency of a band as well as at its overtone. Combination bands are additive in the sense that if a

molecule possesses bands at two different fundamental frequencies, it may show absorption of energy at a frequency equivalent to the sum of these two fundamental frequencies. On the other hand, a Fermi resonance may split an absorption band in two when an overtone frequency exists in the same or similar region as a fundamental frequency. Coupling occurs when adjacent atoms in a molecule have similar frequencies, which lead to a change in overall frequency of the bands. Vibration-rotation bands occur when rotational motion is induced by a vibrational transition (Stuart, 2004).

These complicating factors must be taken in account when selecting or designing an infrared absorption spectroscopy. Fortunately, there is a great variety of components that allows enormous flexibility in the design and configuration of infrared systems. In the next section, we discuss the current and future infrared system component technologies.

When the temperature is above absolute zero all atoms in the molecule undergoes vibrational motion with respect to each other, if the incident radiation has energy that matches the difference in energy between vibrational levels of atoms in the molecules, the molecule will absorb energy and become excited.

There are two types of molecular vibrations, stretching (change in bonds length) and bending (change in bonds angle). The bond can stretch in phase (symmetrical stretching) or out of phase (asymmetric stretching) (Stuart 2004, Griffith & Haseth 2007, Williams 1976).

A polyatomic molecule with N atoms has a total of $(3N)$ degrees of freedom; three of which are translational, and three rotational for nonlinear molecules, while two rotational degrees of freedom for linear molecules. The remaining degrees of freedom are for vibrational motion. They are $3N-6$ for nonlinear molecules and $3N-5$ for linear molecules, as shown in (Table 2.1) (Stuart 2004).

Table 2.1: Molecule degrees of freedom. (Stuart, 2004).

Type of degrees of freedom	Linear	Non linear
Translational	3	3
Rotational	2	3
Vibrational	$3N-5$	$3N-6$
Total	$3N$	$3N$

2.4.2 Quantum mechanical treatment of vibrations

I. **The harmonic oscillator approximation** treats a diatomic as if the nuclei were held together by a spring. The potential energy of classical harmonic oscillator depends upon the square of the displacement from equilibrium and the strength of the spring. All values of energy are allowed classically. The quantum mechanical solution to the harmonic oscillator equation of motion predicts that only certain energies are allowed,

$$E_v = \frac{h}{2\pi} \sqrt{\frac{f}{\pi}} \left(v + \frac{1}{2} \right) \dots \dots \dots (\text{eq.15})$$

The potential energy for diatomic molecule for harmonic oscillator approximation is shown below in figure 2.3

II. **The an-harmonic oscillator** Real molecules do not obey exactly the simple harmonic motion, real bonds do not follow hooks law they are not so elastic. If for example a bond stretches of 60% of its real length then a molecular complicated situation should be assumed The Morse curve, for a molecule undergoing on harmonic extensional compression a purely empirical expression which fits this curve to good approximation was derived by P. Morse and is called the Morse function:

$$E = D_{eq} \left[1 - \exp(a(r_{eq} - r)) \right]^2 \dots \dots \dots (\text{eq.16})$$

a= constant for a particular molecule.
Deq= the dissociation energy.

When it is treated using Schrodinger equation and using

$$E = \frac{1}{2} f (r - r_{eq})^2 \dots \dots \dots (\text{eq.17})$$

then the pattern of the allowed vibration energy levels are found to be

$$E_v = \left(v + \frac{1}{2} \right) \widehat{W}_e - \left(v + \frac{1}{2} \right)^2 W_e X_e \quad \text{cm}^{-1} \quad v = 0,1,2, \dots \dots \dots (\text{eq.18})$$

Where we is an oscillating frequency and \widehat{w}_e is the oscillation frequency in wave number. X_e is the corresponding an-harmonicity constant which is positive and small for bond stretching ($\approx +0.01$) this means that the vibration levels crowded more closely with increasing v (Banwell, C. N 1972).

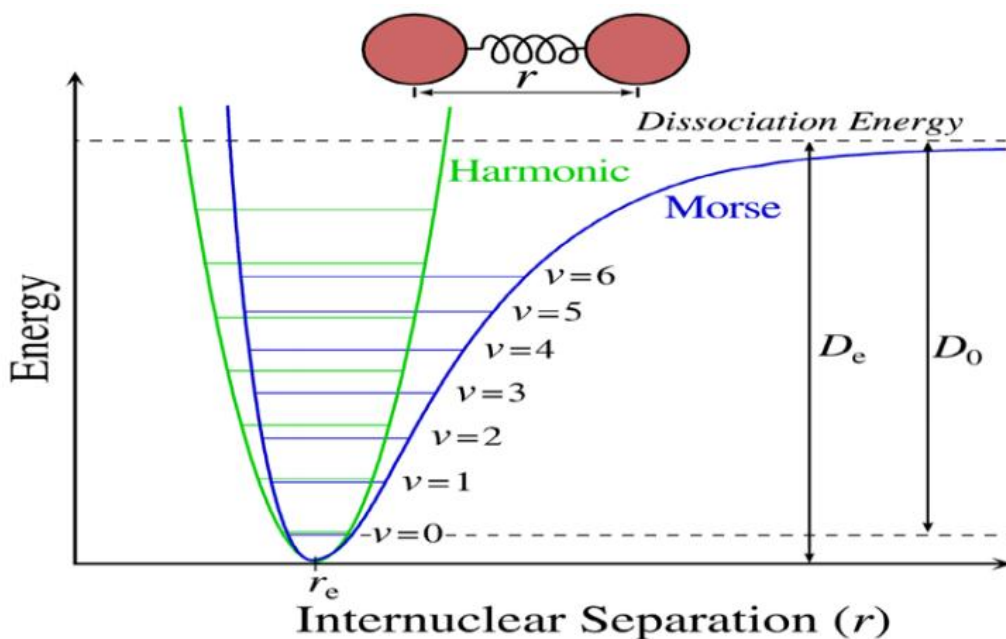


Figure 2.3: potential energy of a diatomic molecule as a function of atomic displacement (inter-nuclear separation) during vibration. The **Morse potential** (blue) and harmonic oscillator potential (green) (Wikipedia: Vibronic spectroscopy).

For many vibrational modes a large number of atoms in the molecule are almost stationary and only few of them have large displacements. The frequency of such mode is characteristic of the functional group of these molecules and it is almost unaffected by other atoms in the molecule, which enabled scientist to assign each absorption band in the infrared region to a typical functional group (Griffith & Haseth 2007). The assigned wave number for each function group is shown in (Table 2.2).

Table 2.2: Typical bond stretching and angel-bending group vibrations (Hollas 2004).

Bond-stretching		Bond-stretching		Angle-bending	
Group	ω/cm^{-1}	Group	ω/cm^{-1}	Group	ω/cm^{-1}
$\text{C}\equiv\text{C}-\text{H}$	3300	$-\text{C}\equiv\text{N}$	2100	$\text{C}\equiv\text{C}-\text{H}$	700
$\text{C}=\text{C}-\text{H}$	3020	$\text{C}-\text{F}$	1100	$\text{C}=\text{C}-\text{H}$	1100
except: $\text{O}=\text{C}-\text{H}$	2800	$\text{C}-\text{Cl}$	650	$\text{C}-\text{H}-\text{H}$	1000
$\text{C}-\text{H}$	2960	$\text{C}-\text{Br}$	560	$\text{C}-\text{H}-\text{H}$	1450
$-\text{C}\equiv\text{C}-$	2050	$\text{Cl}-\text{I}$	500	$\text{C}\equiv\text{C}-\text{C}$	300
$\text{C}=\text{C}$	1650	$-\text{O}-\text{H}$	3600 ^a		
$\text{C}-\text{C}$	900	$\text{N}-\text{H}$	3350		
$\text{Si}-\text{Si}$	430	$\text{P}=\text{O}$	1295		
$\text{C}=\text{O}$	1700	$\text{S}=\text{O}$	1310		

2.5 FT-IR Spectroscopy.

FT-IR spectroscopy is a measurement of wavelength and intensity of the absorption of IR radiation by a sample (Settle, F.A 1997). The old ways of spectroscopy were heavily dependent on dispersion elements such as prisms or gratings so the different components of light (λ , ν) are allowed into the sample separately, while Fourier Transform Spectroscopy allows simultaneous measurements at all frequencies and can be applied to both emission or absorption (Banwell, C. N 1972). Fourier transform spectrometers have greatly extended the capabilities of infrared spectroscopy and have been applied to many areas that are very difficult or nearly impossible to analyze by dispersive instruments (Shernan. M 2014). The most important advantage of FT-IR spectroscopy for biological studies is that spectra of almost any biological system can be obtained in a wide variety of environments (Li et al 2007) .

2.5.1 Infrared (IR) Spectroscopy.

IR spectroscopy is one of the oldest and well established experimental and analytical techniques available to today's scientists (Settle, F. A, 1997) . Simply, it is absorption measurement of different IR frequencies by a sample positioned in the path of an IR beam. The main goal of IR spectroscopic analysis is to determine the chemical functional groups in the sample. Different functional groups absorb characteristic frequencies of IR radiation. Using various sampling accessories, IR spectrometers can accept a wide range of sample types such as gases, liquids and solids. Thus, IR spectroscopy is an important and popular tool for structural elucidation and compound identification (Shernan. M 2014).

2.5.1.1 IR-Region.

Infrared radiation spans a section of the electromagnetic spectrum having wavenumbers from roughly 13,000 to 10 cm^{-1} , or wavelengths from 0.78 to about 1000 μm . It is bound by the red end of the visible region at high frequencies and the microwave region at low frequencies (Shernan. M 2014). IR spectroscopists do not usually use the wavelength to plot their spectra but rather its inverse, wavenumber. Thus, wavenumbers are directly proportional to frequency, as well as the energy of the IR absorption. (Uversky, V. N et al. 2007; Shernan. M 2014). The IR region is commonly divided into three smaller areas: near IR, mid IR and far IR. Mid-IR between 4000 and 400 cm^{-1} is the most frequently used region and it is what we have used in this study. The rough limits for each IR region are shown in the figure 2.4.

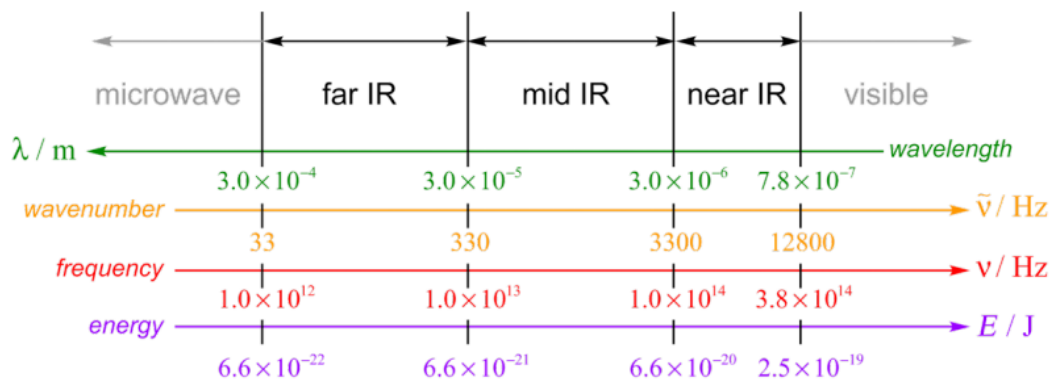


Figure 2.4: Regions of IR spectrum (benjamin-mills.com).

2.5.1.2 IR spectrum presentation.

IR absorption information is generally presented in the form of a spectrum with wavelength or wave-number as the x-axis and absorption intensity or percent transmittance as the y-axis. Transmittance, T , is the ratio of radiant power transmitted by the sample (I) to the radiant power incident on the sample (I_0). Absorbance (A) is the logarithm to the base 10 of the reciprocal of the transmittance (T).

$$A = \log_{10} \left(\frac{1}{T} \right) = -\log_{10}(T) = -\log_{10} \left(\frac{I}{I_0} \right) \dots \dots \dots (\text{eq.19})$$

The transmittance spectra provide better contrast between intensities of strong and weak bands because transmittance ranges from 0 to 100% T whereas absorbance ranges from infinity to zero (Shernan. M 2014).

2.5.1.3 Principle of IR absorption.

Principle of IR absorption by molecules is at the very heart of IR spectroscopy. Absorption is the process by which the energy of a photon is taken up by the matter. There are several types of physical processes that could lie behind absorption, depending on the quantum energy of the particular frequency of EM radiation for example; ionization and electronic transitions. In case of energy absorption, molecules are excited to a higher energy states including IR absorption.

IR radiation does not have enough energy to induce electronic transitions as seen with UV and visible light. It corresponds to energy changes on the order of 8 to 40 KJ/mole. Absorption of IR is restricted to excite vibrational and rotational states of a molecule. Its energy range corresponds to the range encompassing the stretching and bending vibrational frequencies of the bonds in the most covalent molecules.

If the frequency of the radiation matches the vibrational frequency of the molecule then the radiation will be absorbed, causing a change in the amplitude of molecular vibration. However not all bonds in a molecule are capable of absorption infrared

energy only if the vibrations or rotations within a molecule cause a net change in the dipole moment of the molecule then the bond is capable to absorb IR (Pavia, D. L et al. 2009).

Infrared spectrum represents a fingerprint of a sample with absorption peaks which corresponds to the frequencies of vibrations between bonds of the atoms making up the material. Because each different material is a unique combination of atoms, no two compounds produce the exact same infrared spectrum. Therefore, infrared spectroscopy can result in a positive identification (qualitative analysis) of every different kind of material. In addition, the size of the peaks in the spectrum is a direct indication of the amount of material present (quantitative analysis) (Thermo Nicolet, 2001).

The height of the peaks is defined by the Beer-Lambert relationship. It states that the concentration C is directly proportional to the absorbance A.

That is:

$$A = abC \dots \dots \dots \text{(eq.20)}$$

Where (a) is the absorptivity of the molecule and b is the path length or distance that the light travels through the sample (Workman, 1998).

2.5.2 Theory of FT-IR spectroscopy.

Waves can interact with one another, if they come from a similar source or frequency, causing interference effects. Two waves sharing the same frequency with amplitude will interact favourably. Their peaks and troughs will line up and the resultant wave will have amplitude of the summation of the two, known as constructive interference. Two waves interacting out of phase result in destructive interference. One wave's crests will coincide with another wave's troughs and will cancel each other out, resulting in amplitude of zero. The interaction of waves is the key concept of an interferometer (Krishan1975).

An FTIR spectrometer consists of a global light source, a two-beam interferometer (comprised of a fixed mirror, an adjustable mirror and a beam splitter) and a detector, such as mercury cadmium telluride (MCT). Modern interferometers are designed based on the original Michelson interferometer (Fig. 2.5). The Michelson interferometer divides the infrared beam into two paths by use of a beamsplitter which is reflected by two mirrors; one of fixed position and one that moves. The beams are subsequently recombined after path differences have been introduced, creating the opportunity for interference to occur between the beams.

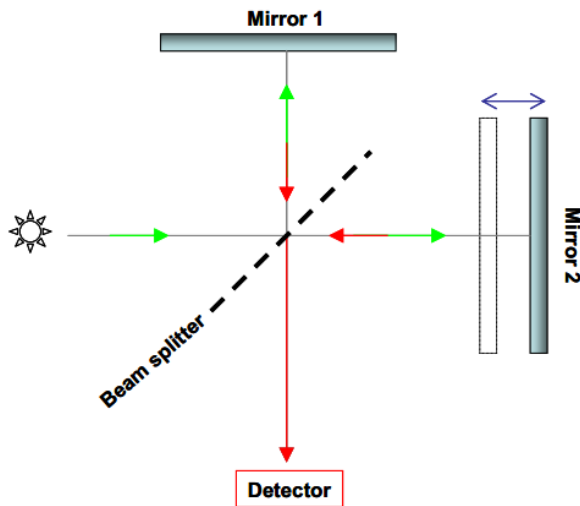


Figure 2.5: Schematic of a Michelson interferometer: The initial IR beam is split by the beamsplitter. The two split beams move different distances and have different phase delays when recombined, hence causing an interference pattern (an interferogram)

The split beams travel to different distances and hence have different phase delays when recombined. The resulting interferogram records the summation of cosine and sine contributions that display the signal intensity as a function of path length. The interferogram is Fourier-transformed which produces the sample spectrogram (Krishan1975).

The interferogram is Fourier transformed with the help of computer to convert the space domain into wave number domain (Viji 2006). The basic integral equation used in FT-IR spectroscopy can be obtained from the definition of Fourier integral theorem. The basic equation used in the case of Michelson interferometer can be derived as follows: Let the amplitude of the wave (travelling in the z-direction) incident on the beam splitter be given as

$$E(z, \nu) d\nu = E_0(\nu) e^{i(\omega t - 2\pi \nu z)} d\nu \dots \dots \dots (\text{eq.21})$$

Where $E_0(\nu)$ is the maximum amplitude of the beam at $z=0$. The amplitude of the beam is divided at the beam splitter and two beams are produced. Let z_1 and z_2 be the distances travelled by the beams when they recombine. Each beam undergoes one reflection from the beam splitter and one transmission through the beam splitter. If r and t are the reflection and transmission coefficients, respectively, of the beam splitter, then the amplitude of the recombined wave E_R is

$$E_R[z_1, z_2, \nu] d\nu = r t E_0(\nu) [e^{i(\omega t - 2\pi \nu z_1)} + e^{i(\omega t - 2\pi \nu z_2)}] d\nu \dots \dots \dots (\text{eq.22})$$

By definition, the intensity after recombination of the beams for the fixed spectral range $d\nu$ is given as

$$\begin{aligned} I(z_1, z_2, \nu) d\nu &= E_R[z_1, z_2, \nu] d\nu E_R^*[z_1, z_2, \nu] d\nu \\ &= 2E_0^2(\nu) |rt|^2 [1 - \cos 2(z_1 - z_2) \nu] d\nu \dots \dots \dots (\text{eq.23}) \end{aligned}$$

And the total intensity at any path difference $x=(z_1-z_2)$ for the whole spectral range is obtained by integrating equation (16) as

$$I_R(x) = 2|rt|^2 \int_0^\infty E_0^2(v)dv + 2|rt|^2 \int_0^\infty E_0^2(v)\cos(2\pi xv)dv.....(eq.24)$$

Fourier cosine transform of equation (17) converts intensity into spectrum as

$$E_0^2(v) = \left(\frac{1}{\pi|rt|^2}\right) \int_0^\infty \left[I_R(x) - \frac{1}{2}I_R(0)\right] \cos(2\pi vx) dx.....(eq.25)$$

In the above equation, $I_R(0)$ represents the flux associated with waves at zero arm displacement where the waves for all frequencies interact coherently. Thus, $I_R(0)$ is the flux associated with coherent interference and $I_R(x)$ is the flux associated at path difference x . $\left[I_R(x) - \frac{1}{2}I_R(0)\right]$ is called the interferogram.

The spectrum $S(v)$, which is proportional to $E_0^2(v)$ can be given from equation (18) as

$$S(v) \propto E_0^2(v) = constant \int_0^\infty \left[I_R(x) - \frac{1}{2}I_R(0)\right] \cos(2\pi vx) dx.....(eq.26)$$

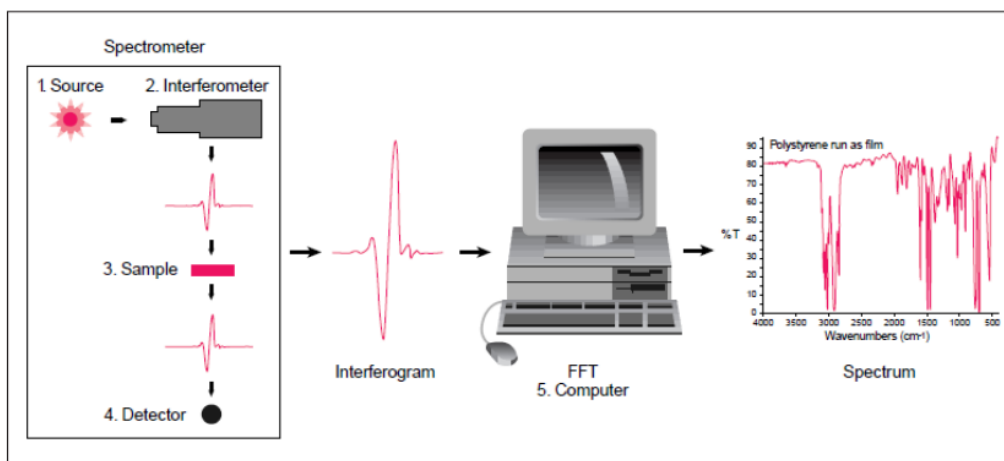
The interferogram is Fourier transformed with the help of computer to convert the space domain into the wave number domain (Cooper, A 2004).

2.5.3 The sample analysis process by FT-IR spectrometer.

The normal instrumental process is as follows:

The Source: Infrared energy is emitted from a glowing black-body source. This beam passes through an aperture which controls the amount of energy delivered to the sample (and, ultimately, to the detector). **The Interferometer:** The beam enters the interferometer where the “spectral encoding” takes place. The resulting interferogram signal then exits the interferometer. **The Sample:** The beam enters the sample compartment where it is transmitted through or reflected off of the surface of the sample, depending on the type of analysis being accomplished. This is where specific frequencies of energy, which are uniquely characteristic of the sample, are absorbed. **The Detector:** The beam finally passes to the detector for final measurement. The detectors used are specially designed to measure the special interferogram signal. **The Computer:** The measured signal is digitized and sent to the computer where the Fourier transformation takes place. The final infrared spectrum is then presented to the user for interpretation and any further manipulation (Thermo Nicolet 2001).

Figure 2.6: FT-IR spectrometer layout and basic components (chemwiki.ucdavis.edu)



2.6 Ultraviolet-Visible (UV-VIS) Spectrophotometer.

This absorption spectroscopy uses electromagnetic radiations between 190nm to 800 nm and is divided into the ultraviolet (UV 190-400 nm) and visible (VIS 400- 800 nm) regions. Since the absorption of ultraviolet or visible radiation by a molecule leads transition among electronic energy levels of the molecule. It is also often called as electronic spectroscopy.

Nature of electronic transitions.

Energy absorbed in the UV regions produces changes in the electronic energy of the molecule. As a molecule absorbs energy, an electron is promoted from an occupied molecular orbital (usually a non-bonding or bonding π orbital) to an unoccupied molecular orbital (an anti-bonding π^* or σ^* orbital) of greater potential energy, as in figure 2.7.

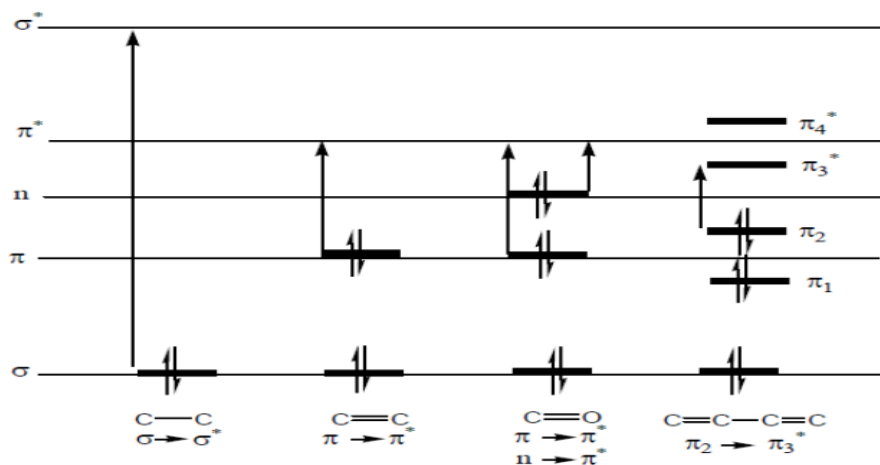


Figure 2.7: Relative energies of orbitals most commonly involved in electronic spectroscopy of organic molecules (Prof. Subodh Kumar. 2006).

For most molecules, the lowest energy occupied molecular orbitals are σ orbitals, which correspond to σ bonds. So the possible electronic transitions are:

$$n \rightarrow \pi^* < n \rightarrow \sigma^* < \pi \rightarrow \pi^* < \sigma \rightarrow \pi^* < \sigma \rightarrow \sigma^*$$

The energy of radiation being absorbed during excitation of electrons from ground state to excited state primarily depends on the nuclei that hold the electrons together in a bond. The group of atoms containing electrons responsible for the absorption is called chromophore (Hildebrandt, P & Siebert, F 2008).

2.7 Fluorescence Spectrophotometer.

Fluorescence spectrophotometry is a class of techniques that assay the state of a biological system by studying its interactions with fluorescent probe molecules (Dong, C. Y & So, P. T 2002). Luminescence is emission of light by a substance not resulting from heat; it is thus a form of cold body radiation. Luminescence is formally divided into two categories fluorescence and phosphorescence depending on the nature of the excited states (Soukpo'e-Kossi et al 2007).

Fluorescence and phosphorescence are photon emission processes that occur during molecular relaxation from electronic excited states. Fluorescence is that process in which the emission of light by a substance that has absorbed light or other electromagnetic radiation (Johnson. L & Spence. T. Z. M 2010). A fluorophore is a molecule that is capable of fluorescing. In its ground state, the fluorophore molecule is in a relatively low energy, stable configuration, and it does not fluoresce. Fluorophore is unstable at high energy configurations, so it eventually adopts the lowest-energy excited state, which is semi-stable.

The process responsible for the fluorescence of fluorescent probes and other fluorophores is illustrated by the simple electronic-state diagram (Jablonski diagram) shown in Figure (2.8) below

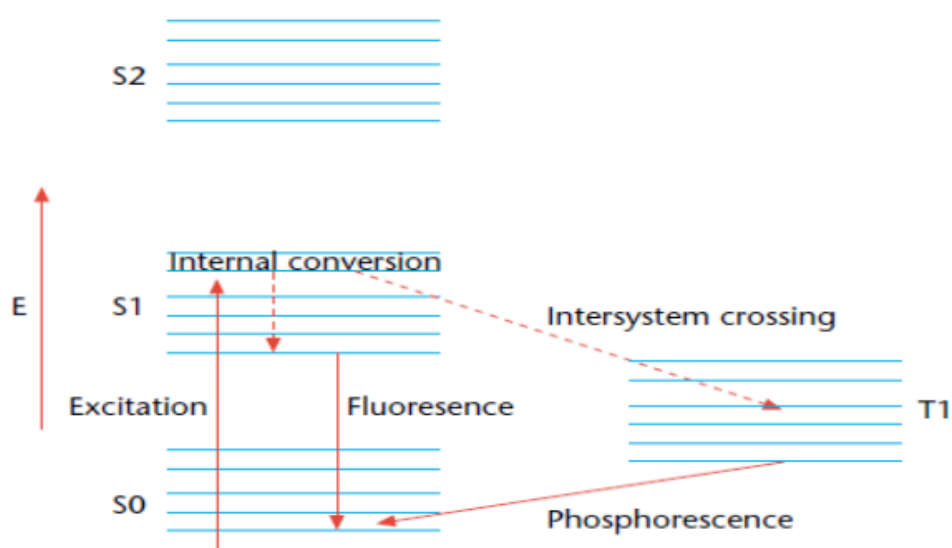


Figure 2.8: The Jablonski diagram of fluorophore excitation (Dong, C.Y & So, P.T 2002).

Where E denotes the energy scale; S₀ is the ground singlet electronic state, S₁ and S₂ are the successively higher energy excited singlet electronic states. T₁ is the lowest energy triplet state (Dong, C.Y & So, P.T 2002).

The fluorescence lifetime and quantum yield are the most important characteristics of a fluorophore. Quantum yield is the number of emitted photons relative to the number of absorbed photons. The lifetime is determined by the time available for the fluorophore to interact with or diffuse in its environment, and hence the information available from its emission (Iakowicz 2006).

Fluorophores are divided into two main classes. First intrinsic fluorophores are those that occur naturally, such as aromatic amino acids. Secondly extrinsic fluorophore are added to the sample to provide fluorescence when none exists, or to change the spectral properties of the sample (Iakowicz 2006).

After the excitation occurs, the excited state exists for a finite time (typically 1-10 nanoseconds). During this time; the fluorophore undergoes conformational changes and is also subject to a multitude of possible interactions with its molecular environment. These processes have two important consequences. First, the energy of S₂ is partially dissipated, yielding a relaxed singlet excited state (S₁) from which fluorescence emission originates. Second, not all the molecules initially excited by absorption return to the ground state (S₀) by fluorescence emission.

At **Fluorescence Emission stage** a photon of energy $h\nu_{EM}$ is emitted, returning the fluorophore to its ground state S₀. Due to energy dissipation during the excited-state lifetime, the energy of this photon is lower, and therefore of longer wavelength, than

the excitation photon $h\nu_{EX}$. The difference in energy or wavelength represented by $(h\nu_{EX} - h\nu_{EM})$ is called the Stokes shift (Johnson, L & Spence, T. Z. M 2010).

2.8: Quenching.

Decrease of fluorescence intensity by interaction of the excited state of the fluorophores with its surroundings is known as quenching and is relatively rare. Quenching can occur in several mechanisms, collisional quenching occurs when excited state fluorophores are deactivated upon contact with some other molecule in solution, which is called quencher (Sheehan 2009). For collisional quenching the decrease in intensity is given by Stern-Volmer equation:

$$\frac{F_0}{F} = 1 + K[l] = 1 + K_q\tau_0[l] \dots\dots\dots(\text{eq.27})$$

Where K is Stern-Volmer quenching constant, K_q is biomolecular quenching constant, τ_0 is the unquenched lifetime, and l is the quencher concentration. The quenching constant indicates the sensitivity of the fluorophores to the quencher. There are a wide variety of molecules that acts as a collisional quencher such as oxygen, halogen, amines, and electrondeficient molecules like acrylamide. Quenching mechanism differ according to fluorophores quencher pair, for instance quenching of indole by acrylamide occur as a result of electron transfer from indole to acrylamide, while quenching by halogens and heavy atoms occurs as a result of spin orbit coupling and intersystem crossing to the triplet state (Lakowicz, 2006, Sheehan 2009). Static quenching is another type of quenching. It occur in the ground state and does not rely on diffusion or molecular collisions. It occurs as a result of complex formation in the ground state between fluorophores and quencher (Turro, 1991).

Chapter three:

Experimental part

Chapter three

In this chapter experimental procedure has been discussed in details including sample preparation for FTIR, UV-vis spectroscopy, and fluorescence spectroscopy.

The instrumentation of Fluorospectrometer (NanoDrop 3300), UV-vis spectrometer (NanoDrop1000), Bruker IFS 66/S . The experimental procedure followed in this research has been explained.

3.1 samples preparations.

1-Stearoyl-2-oleoyl-sn-glycero-3-phosphocholine (SOPC, 99 % pure, MW = 788.145 g/mol) with the chemical formula ($C_{44}H_{86}NO_8P$) , digitonin with the chemical formula ($C_{56}H_{92}O_{29}$) (MW = 1229.323 g/mol) , phosphate buffered saline (2.7 mM KCl and 137 mM NaCl, pH 7.4) and chloroform were used to prepare the samples. All above chemicals were purchased from Sigma Aldrich Company and used without further purification. Optical grade silicon windows (NICODOM Ltd) were used as spectroscopic cell windows. These windows were purchased from Sigma Aldrich Company.

FTIR measurements were carried out using several samples in the form of thin films of 1-Stearoyl-2-oleoyl-sn-glycero-3-phosphocholine, and digitonin solutions. UV-vis and fluorescence measurements were done using the liquid samples of the mentioned solutions.

3.1.1 Preparation of SOPC stock solution.

SOPC was dissolved in chloroform, to a concentration of (50 mg/ml), 2.5mg from stock solution was evaporated and dissolved in 2.5ml PBS to get a final concentration of (1mg/ml) solution.

To get small vesicles of SOPC ,incubation process and freezing – thawing cycle must using in this research .

3.1.2 Preparation of digitonin stock solution.

100 mg of digitonin was dissolved in 67.78 ml of PBS to prepare 1.2 mM stock solution. Different concentrations of digitonin (0.6, 0.5,0.4,0.3,0.2 and 0.1 mM) were prepared in PBS solution using molarity dilution equation.

3.1.3 SOPC - digitonin solutions.

The final concentrations of SOPC-digitonin solutions were prepared by mixing 20 μ l of SOPC and 4 μ l of digitonin. SOPC concentration in all samples kept at 1 mg/ml. However, the final concentrations of digitonin in solutions are (0.6,0.5, 0.4, 0.3, 0.2 and 0.1mM).

3.1.4 Thin film preparation.

After cleaning silicon windows very well, 24 μL of each sample were applied on a certain area on the silicon window plate and left to dry at room temperature inside the incubator for 24 hours. The dehydrated films are prepared with the desired concentration of SOPC and digitonin . to obtain a transparent thin film on the silicon window. All solutions were prepared at the same time at room temperature. For background measurement, a clean silicon window has been kept in the same incubator together with the rest of samples, in order to have all samples in the same environment.

3.2 Instruments.

Many instruments can be used in studying the interaction of SOPC and digitonin . In this work the following instruments have been used in taking the measurements.

3.2.1. Fluorospectrometer (NanoDrop 3300).

Fluorescence measurements had been done using Fluorospectrometer (NanoDrop ND-3300) at 25°C. The excitation source comes from one of three solid-state light emitting diodes (LED's), which are oriented 90° to the detector. A 2048-element CCD array detector, covering 400 –750 nm, is connected by an optical fiber to the optical measurement surface. The spectrometer is configured with a cut filter to eliminate light transmission below 395 nm.

A 1-2 μl sample was pipetted onto the end of the lower measurement pedestal (the receiving fiber). A non-reflective “bushing” attached to the arm is then brought into contact with the liquid sample causing the liquid to bridge the gap between it and the receiving fiber. The gap, or path length, is controlled to 1mm. Following excitation with one of the three LEDs, emitted light from the sample passing through the receiving fiber is captured by the spectrometer. The NanoDrop 3300 is controlled by software run from a PC. The image below lists some of common fluorophores that can be measured using the NanoDrop 3300 along with the most appropriate excitation LED.

The excitation source option includes the UV-LED with maximum excitation at 365nm, the blue-LED with maximum excitation at 470nm, and the white-LED in the range 500-650nm.

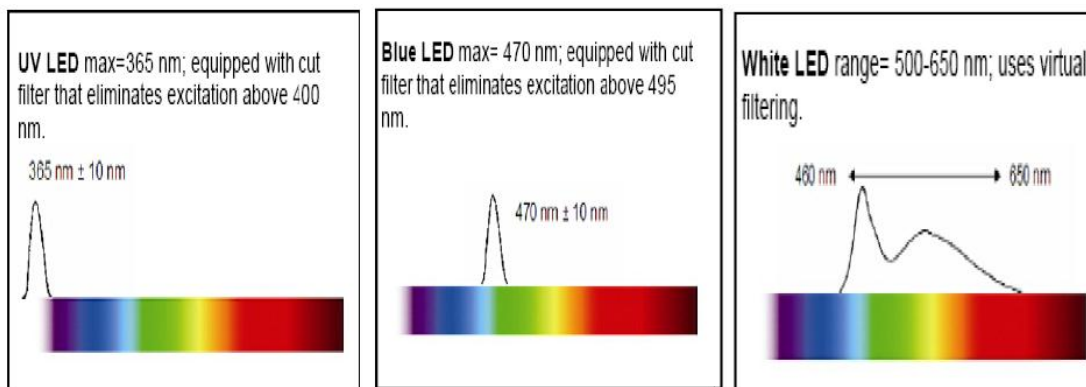


Figure 3.1:Excitation LEDs.

3.2.2. UV-VIS spectrophotometer (NanoDrop ND-1000).

The Thermo Scientific NanoDrop 1000 Spectrophotometer measures 1 µl samples with high accuracy and reproducibility. The full spectrum (220nm-750nm) spectrophotometer utilizes sample retention technology that employs surface tension alone to hold the sample in place. This eliminates the need for cumbersome cuvettes and other sample containment devices and allows for clean up in seconds. In addition, the NanoDrop 1000 Spectrophotometer has the capability to measure highly concentrated samples without dilution (50X higher concentration than the samples measured by a standard cuvette spectrophotometer).

The sample was pipetted at the end of a fiber optic cable, and then a second fiber optic cable is brought in contact with the sample causing the liquid to bridge the gap between the fiber optic ends which is controlled between 1-0.2mm. A pulsed xenon flash lamp provides the light source that pass through the sample. The excitation is made at 210nm and emission occurs at 280nm. The sample size is not critical but the liquid column must be formed so that the gap between the upper and lower pedestals is bridged with the sample.

3.2.3. Fourier Transform Infrared Spectroscopy (FTIR).

The FTIR measurements were obtained on Bruker IFS 66/S spectrophotometer, equipped with liquid nitrogen –cooled MCT detector and a KBr beam splitter the spectrometer was continuously purged with dry air during measurement. The absorption spectrums in the mid infrared region (4000-400 cm⁻¹) were taken and measured. Because of the need to a relative scale for the absorption intensity, a background spectrum must also be measured. This is normally a measurement with no sample in the beam.

The two most popular detectors for a FTIR spectrometer are deuterated triglycine sulfate (DTGS) which is a pyroelectric detector that delivers rapid responses because it measures the changes in temperature rather than the value of temperature, and “our detector” mercury cadmium telluride (MCT) which is a photon (or quantum) detector that depends on the quantum nature of radiation and also exhibits very fast responses.

It must be maintained at liquid nitrogen temperature (77 °K) to be effective. Generally MCT detectors are faster more sensitive than DTGS detectors.

3.3 Experimental Procedures:

3.3.1. Fluorospectrometer procedure:

The prepared liquid samples of SOPC free and SOPC-digitonin solutions were used to make the fluorescence Measurements in the following steps:

With the sampling arm open, pipette the sample onto the lower measurement pedestal.



Close the sampling arm and initiate a measurement using the operating software on the PC. The sample column is automatically drawn between the upper bushing and the lower measurement pedestal and the measurement is made.



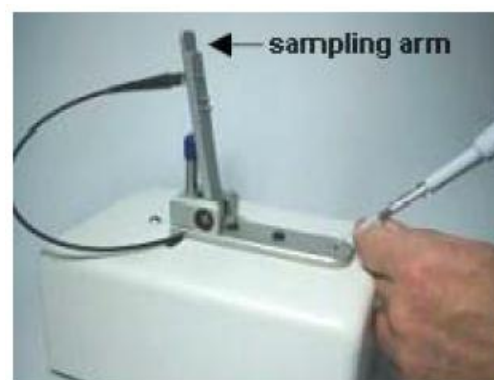
When the measurement is complete, open the sampling arm and blot the sample from both the upper bushing and the lower pedestal using low lint laboratory wipe to prevent sample carryover and avoid residue buildup



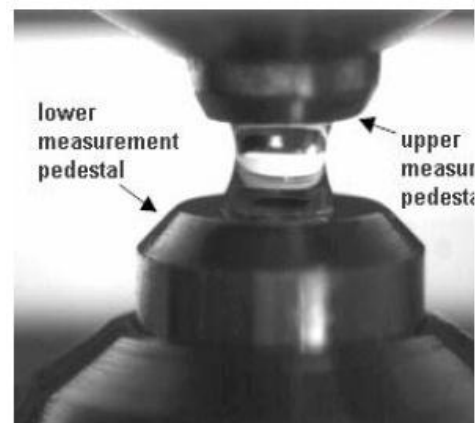
3.3.2. UV-VIS spectrometer (ND-1000):

The same samples used in UV-vis measurements were used following these steps:

With the sampling arm open, pipette the sample onto the lower measurement pedestal.



Close the sampling arm and initiate a spectral measurement using the operating software on the PC. The sample column is automatically drawn between the upper and lower measurement pedestals and the spectral measurement made.



When the measurement is complete, open the sampling arm and wipe the sample from both the upper and lower pedestals using a soft laboratory wipe. Simple wiping prevents sample carryover in successive measurements.



When the NanoDrop ND-1000 and NanoDrop ND-3300 spectrophotometers are blanked, a spectrum is taken for the reference material, and stored in computer memory as an array of light intensities by wavelength. When a measurement of a sample is taken the intensity of light that has been transmitted through the sample is recorded, and then the sample intensity with the blank intensity was used to calculate the sample absorbance according to the following equation:

$$\text{Absorbance} = A = -\log \left(\frac{\text{Intensity sample}}{\text{Intensity blank}} \right)$$

Both the intensity of the blank and of the sample is needed to give the absorbance at a given wavelength.

3.3.3. Fourier Transform infrared (FTIR) spectroscopy.

The nitrogen gas cylinder is switched on by turning the switch on the top of the cylinder anticlockwise. When the gas reaches the mirror then a green led will start flashing at the base of the spectrometer. Liquid nitrogen must be employed inside the instrument and the prepared samples then can be delivered starting with the background sample.

Each measurement is taken at a resolution of 4 cm^{-1} and an average 60 scans to increase signal to noise ratio, the aperture used in this study was 8mm, since it has been founded that this aperture gives best signal to noise ratio. Many manipulation techniques have been performed on all the spectra by OPUS software (Optic User Software) such as baseline correction, normalization, and peak areas calculations. The peak positions were determined using second derivative of the spectra.

For temperature dependence study SOPC-digitonin complexes on silicon windows were placed into an infrared cell window. The temperature of the cell was controlled by an external water path and was increased gradually from 20⁰C to 80⁰C at 3⁰C per 5

minutes scan rate. Peak positions were determined using second derivative at 9 smoothing points by OPUS software, calculation of areas under the different curves were performed using Fourier self deconvolution (FSD) techniques by OPUS software.

The advantages of the FTIR instrument is the high speed and sensitivity, as it acquire the interferogram in less than a second. Modern FTIR spectrometers have a powerful computerized data system, as it can perform many data processing tasks (Jilie Kong, 2007), a brief explanation of these tasks is given below:

1. Baseline correction:

The offset correction is performed by selecting a single point of multiple points on a spectrum and adding to them or subtract a y-value to correct the baseline offset. This processing step is used to bring the minimum point to zero, or to align the baseline of two or more spectra causing them to overlap.

2. Derivatives:

Derivatives are used to remove offset and slope due to background differences. In our study we have used second derivative to determine the positions of peaks.

3. Fourier self deconvolution:

It is the band narrowing technique that is most widely used in infrared spectroscopy of biological material. The aim of FSD is to enhance the apparent resolution of a spectrum, or to decrease the line width. So the broad and overlapping lines of spectrum can be separated into sharp single lines.

The deconvolution correspond to a multiplication of the interferogram $I(x)$ using the exp^{ax} deconvolution function for Lorentzian and exp^{ax^2} for Gaussian shapes, which will intensifies the interferogram edges.

The deconvolution factor is the maximum value of these functions at the end of the interferogram, deconvolution factors of 100, 1000, and 5000 correspond to a maximum amplification of 3.4, 12.8, and 40 in the case of Lorentzian shape, and 1.06, 3.2, and 16 in the case of Gaussian shapes. If you work with Lorentzian shapes it is recommended to increase the deconvolution factor in the order of 50, 100, 1000, 5000, and to stop if the resultant spectrum shows artificial oscillations (Bruker, 2004). Successful application of FSD will enhance peak separation on overlapping absorption bands.

4. Curve fitting:

The curve fitting command allows calculating single components in a system of overlapping bands, a model that consists of an estimated number of bands. A baseline should be generated before the fitting calculation is started. The model can be set up interactively on the display and is optimized during the calculation (Bruker, 2004).

Chapter Four:
Results and Discussion

Results and Discussion.

This chapter includes the main results, analysis and discussions of our data. In the first section, UV-VIS spectrophotometer results are discussed and analyzed. The next section deals with fluorescence spectrophotometer results. In the final section, FT-IR graphs and data analysis are given.

4.1 UV-absorption spectroscopy:

UV-absorption spectroscopy was used to determine the binding constants between SOPC and digitonin. The strength of interaction between SOPC and digitonin is dependent on the binding constant which can be calculated using graphical analysis of the absorbance spectrum.

The absorption spectra for SOPC and digitonin with different concentrations of digitonin were recorded and shown in (Fig 4.1). The excitation has been done at 210 nm, while the absorption is recorded at 280 nm. The UV absorbance intensity of SOPC has decreased with increasing digitonin concentration.

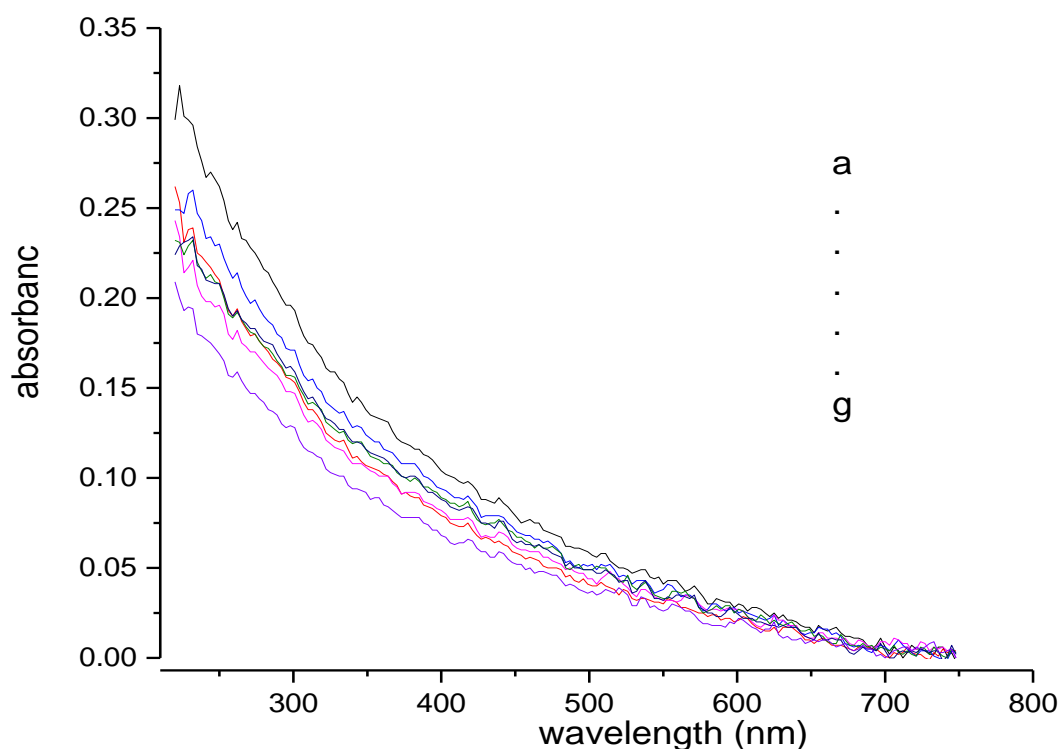


Figure 4.1: UV absorbance spectra of SOPC-digtonin complexes at different digitonin concentrations (a: 0.0mM, b: 0.1mM, c: 0.2mM, d: 0.3mM, e: 0.4mM, f:0.5mM, and g:0.6mM)

4.1.1. Determination of binding constants (K) by UV absorption spectroscopy:

To determine the binding constant (k) by UV-Vis. spectroscopy a plot of $\frac{1}{A-A_0}$ VS $\frac{1}{L}$ is made. This plot indicates a linear relation and the binding constant (k) is found by taking the ratio of the intercept to the slope, which can be seen clearly from the following equation (Darwish et al. 2012).

$$\frac{1}{(A - A_0)} = \frac{1}{(A_\infty - A_0)} + \frac{1}{K(A_\infty - A_0)} \frac{1}{L}$$

Where A_0 corresponds to the absorption of SOPC at 280nm in the absence of digitonin, while A_∞ is the final absorption of SOPC after it binds to the digitonin, and A is the recorded absorption at the different concentrations of the digitonin.

A plot of $\frac{1}{A-A_0}$ VS $\frac{1}{L}$ for different concentrations of digitonin in SOPC-digitonin complexes is shown in (Fig. 4.2).

The binding constant for SOPC-digitonin is calculated to be $5.324 \times 10^3 M^{-1}$

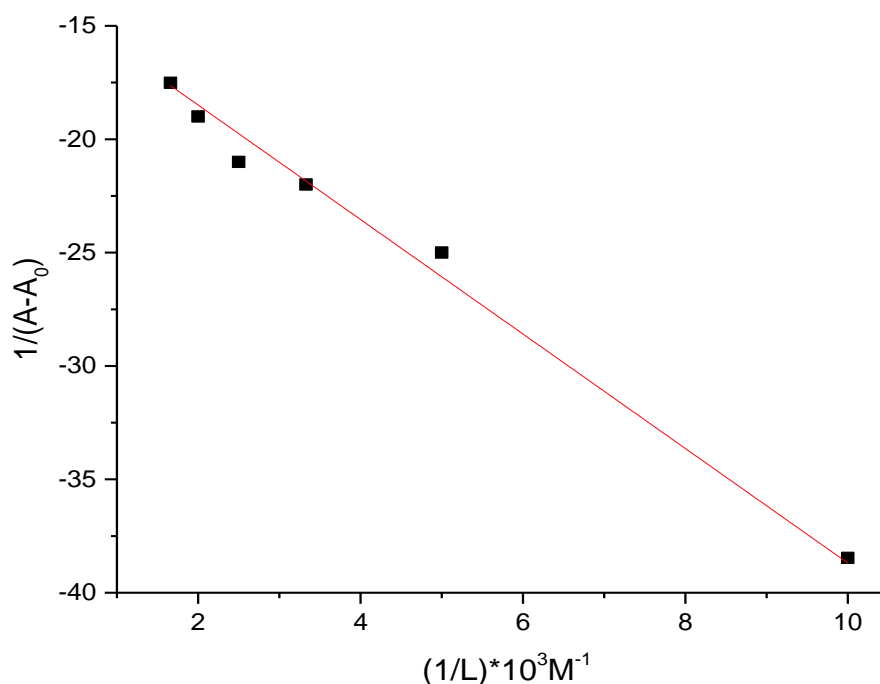


Figure 4.2: the plot of $\frac{1}{A-A_0}$ VS $\frac{1}{L}$ for SOPC with different concentrations of digitonin.

4.2 Fluorescence spectroscopy:

Fluorescence spectroscopy can be applied to a wide range of problems in the chemical and biological sciences. The measurements can provide information on a wide range of molecular processes, including the interactions of solvent molecules with fluorophores, conformational changes, and binding interactions (Lakowicz 2006).

Various molecular interactions can decrease the fluorescence intensity of a compound such as molecular rearrangements, excited state reactions, energy transfer, ground state complex formation, and collisional quenching (Turro 1991, Sheehan 2009). The emission occurs at 439 nm.

The fluorescence emission spectra of SOPC with various concentrations of digitonin (0.1, 0.2, 0.3, 0.4, 0.5, and 0.6 mM) are shown in (Fig 4.3).

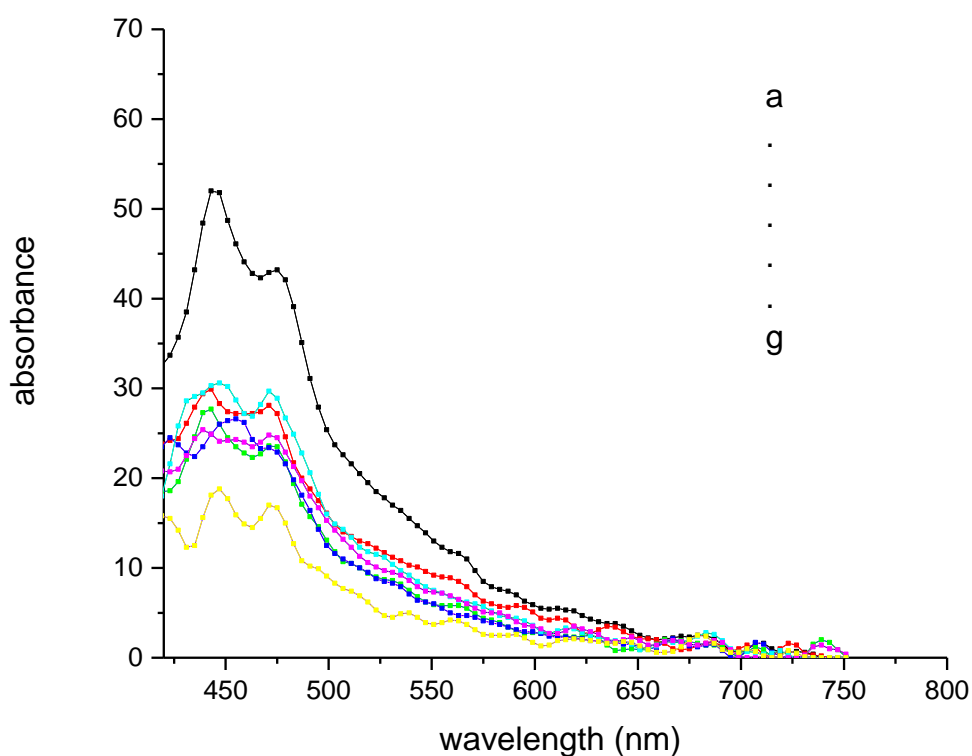


Figure 4.3: The fluorescence emission spectra of SOPC with various concentrations of digitonin (0.1, 0.2, 0.3, 0.4, 0.5, and 0.6 mM).

4.2.1. Determination of Stern-Volmer quenching constants (K_{sv}) and the quenching rate constant (K_q):

Fluorescence quenching can be induced by different mechanisms that were usually classified into static quenching and dynamic quenching. Dynamic quenching arises from collisional encounters between the fluorophores and quenchers while static quenching results from the formation of a ground state complex between the fluorophores and the quenchers (Turro1991).

For dynamic quenching, the decrease in fluorescence intensity is described by Stern-Volmer equation (Lakowicz 2006, Sheehan 2009).

$$\frac{F_0}{F} = 1 + K_{sv}[L] = 1 + K_q\tau_0[L]$$

Where F and F_0 are the fluorescence intensities with and without quencher, K_q is the quenching rate constant, K_{sv} is the Stern-Volmer quenching constant, $[L]$ is the concentration of digitonin, and τ_0 is the average lifetime of the biomolecule without quencher.

The Stern-Volmer quenching constants K_{sv} were obtained by finding the slope of the linear curve obtained when plotting $\frac{F_0}{F}$ vs $[L]$. The quenching rate constant K_q can be calculated using the fluorescence lifetime of digitonin to be 1.1ns .

The plots of $\frac{F_0}{F}$ vs $[L]$ for SOPC-digitonin complexes are shown in (Fig 4.4). From these plots the Stern-Volmer quenching constant was found to be $1.05 \times 10^3 \text{ Lmol}^{-1}$. The quenching rate constants SOPC-digitonin were then calculated to be $1.05 \times 10^{11} \text{ Lmol}^{-1}\text{s}^{-1}$.

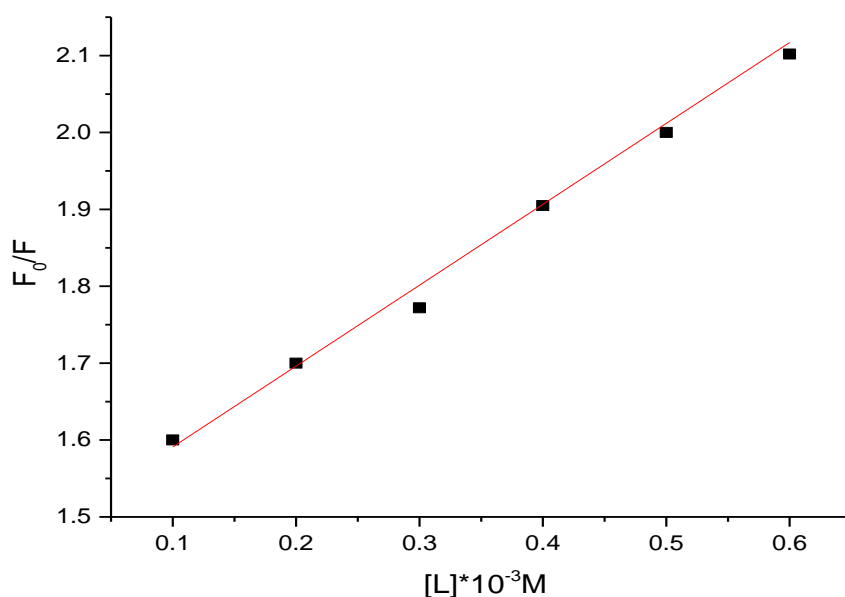


(Fig 4.4):The plots of $\frac{F_0}{F}$ vs $[L]$ for SOPC-digitonin complexes

4.2.2. Determination of the binding constants (K) by fluorescence spectroscopy:

For static quenching, the following equation is used to determine the binding constant between SOPC and digitonin.

$$\frac{1}{F_0 - F} = \frac{1}{F_0 K(L)} + \frac{1}{F_0}$$

Where K is the binding constant of digitonin with SOPC. To determine the binding constants of SOPC-digitonin systems, a plot of $\frac{1}{F_0 - F}$ vs $\frac{1}{L}$ for different digitonin concentrations is made. The plots are linear and have a slope of $\frac{1}{F_0 K}$ and intercept $\frac{1}{F_0}$

According to the above equation. By taking the quotient of the intercept and the slope, the binding constants K(L) can be calculated.

The plot of $\frac{1}{F_0 - F}$ vs $\frac{1}{L}$ for SOPC-digitonin complexes are shown in (Fig 4.5). The binding constants calculated from the slope and the intercept in (Fig. 4.5) and are found to be $5.191 \times 10^3 M^{-1}$

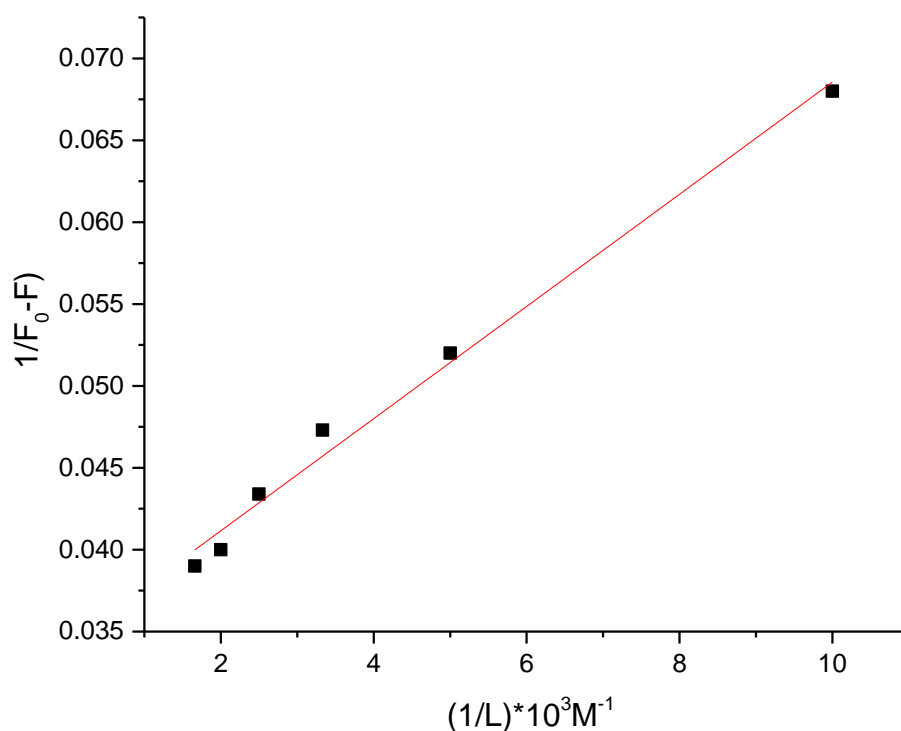


(Fig 4.5):The plot of $\frac{1}{F_0 - F}$ vs $\frac{1}{L}$ for SOPC-digitonin

4.3 Fourier transform infrared (FTIR) spectroscopy:

FT-IR transform spectrophotometers have greatly extended the capabilities of infrared spectroscopy and have been applied to many areas that are very difficult or nearly impossible to analyze by dispersive instruments (Shernan 2014). The infrared of the lipids is characterized by a set of absorption regions known bands,

Infrared spectrum of an aqueous suspension of a typical membrane lipid, 1-Stearyl-2-oleoyl-*sn*-glycero-3-phosphocholine (SOPC), in the range $3000\text{--}1000\text{cm}^{-1}$. The three regions of study corresponding to the hydrophobic region (CH_2 stretching), the interfacial region ($\text{C}=\text{O}$ stretching) and the polar region ($\text{P-O}2^-$ stretching) are depicted in the (Fig 4.6).

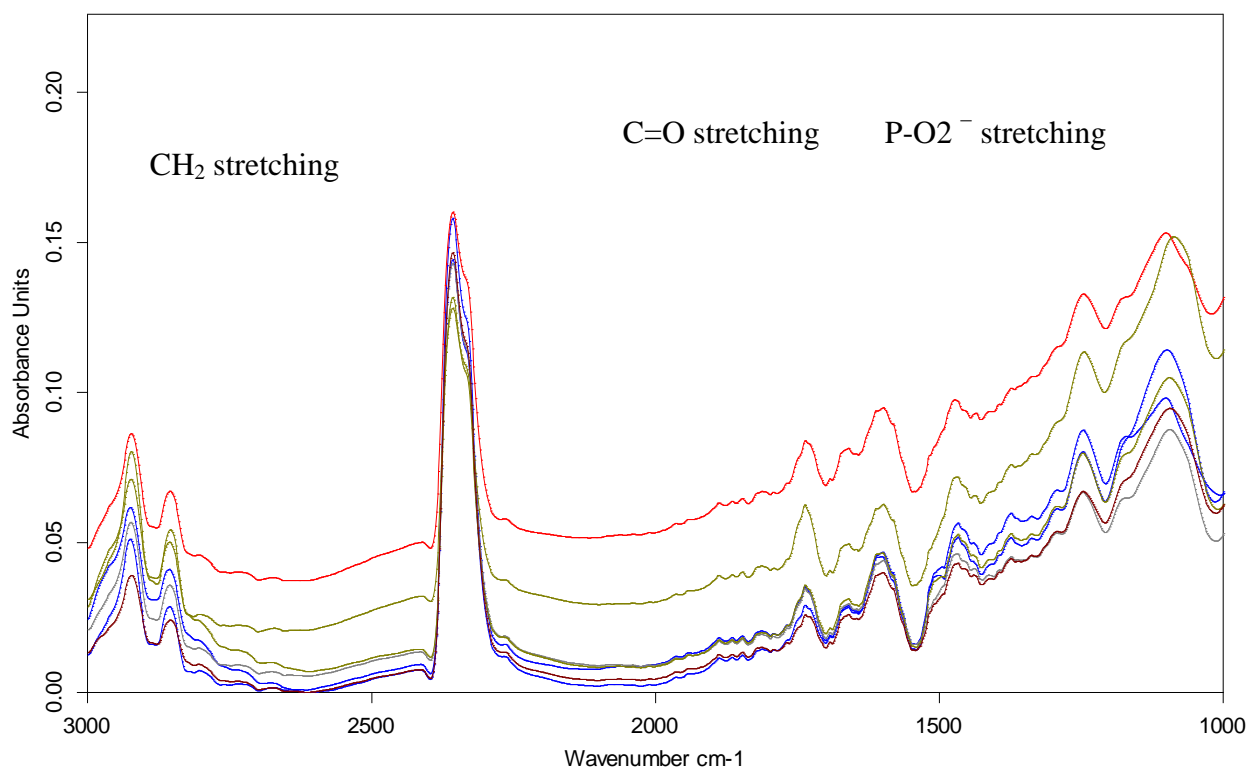


(Figure 4.6):the hydrophobic region (CH_2 stretching), the interfacial region ($\text{C}=\text{O}$ stretching) and the polar region ($\text{P-O}2^-$ stretching) are depicted in the.

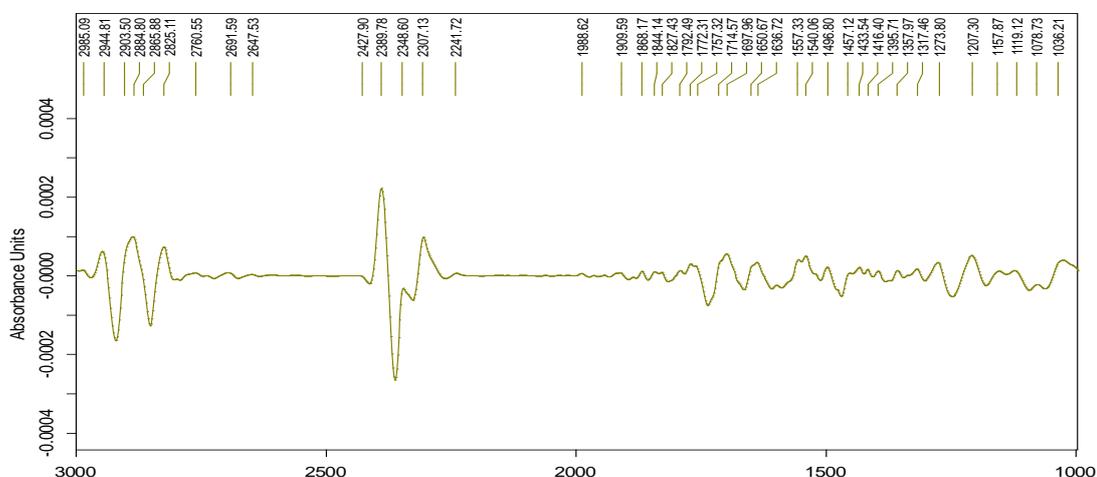
These bands were tentatively identified on the basis of reference standards and published FTIR spectra in relation to specific molecular groups. The results were interpreted (Table 4.1)(Fringeli and Gunthard., 1981; Casal and Mantsch, 1984; Lee and Chapman, 1986; Mantsch and McElhaney,1991).

Table 4.1: The bands were tentatively identified on the basis of reference standards and published FTIR spectra in relation to specific molecular groups.

S. No.	Frequency in wavelength, in cm^{-1}	Assignment of vibration
1-	2957	CH_3 stretching, asymmetric
2-	2924	CH_2 stretching, asymmetric
3-	2871	CH_3 stretching, symmetric
4-	2853	CH_2 stretching, symmetric
5-	1732	$\text{C}=\text{O}$ stretching, esters
6-	1467	CH_2 bending, scissoring ($\text{Lc}+\text{L}_\beta$ gel phase)
7-	1456	CH_2 bending, scissoring ($\text{Lc}+\text{L}_\beta$ gel phase)
8-	1402	sn-1, α - CH_2 bending, scissoring
9-	1380	CH_3 bending, deformation, symmetric
10-	1233	PO_2^- stretching, asymmetric
11-	1171	$\text{C}-\text{O}$ stretching, single bond
12-	1159	$\text{C}-\text{C}$ stretching, skeletal
13-	1060	$\text{R}-\text{O}-\text{P}-\text{O}-\text{R}$
14-	1082	PO_2^- stretching, symmetric

4.3.1. Peak positions:

The second derivative technique and Fourier self deconvolution (FSD) can be used to obtain the peaks positions of the FTIR spectrum. The second derivative of the FTIR spectrum for SOPC free in The three regions are shown in (Fig 4.7), and The FTIR spectra of SOPC-dgintonin thin films with concentrations (0.1, 0.2, 0.3, 0.4, 0.5 and 0.6mM) are shown in (Fig 4.8).



(Fig 4.7) :The second derivative of the FTIR spectrum for SOPC free in The three regions.

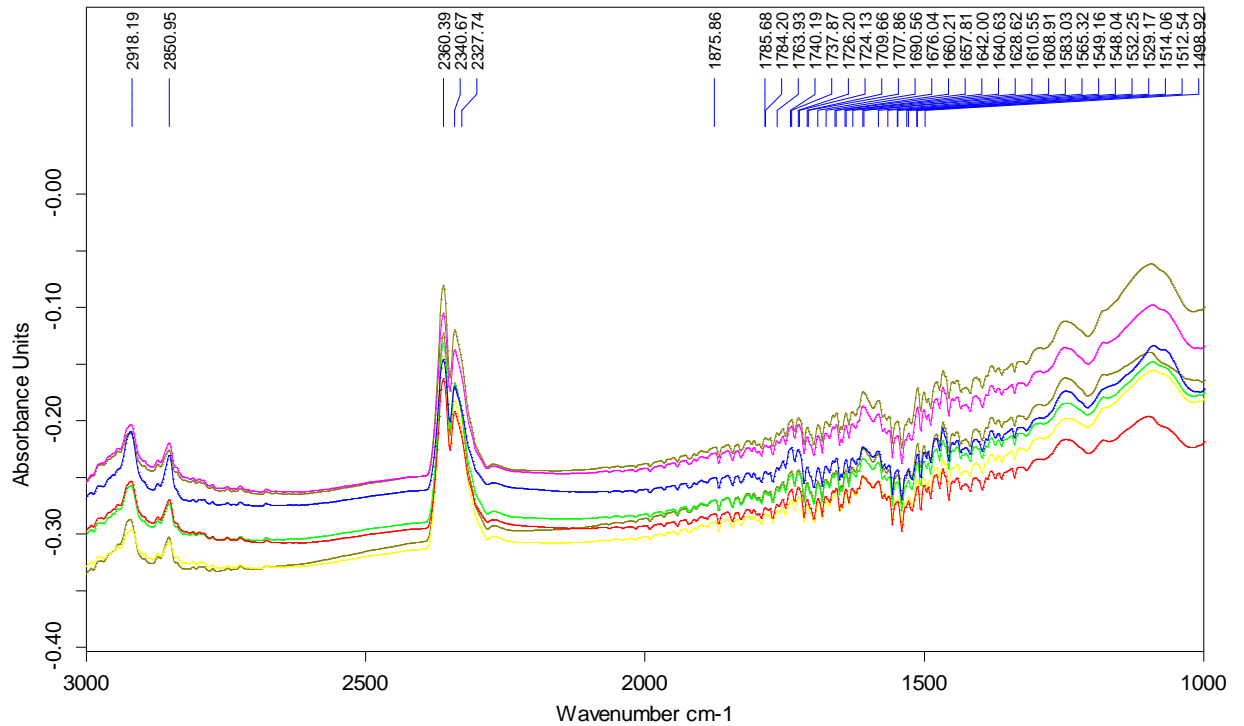


(Fig 4.8) :The FTIR spectra of SOPC-dgitonin thin films with concentrations (0.1, 0.2, 0.3, 0.4, 0.5 and 0.6mM)

The second derivative of the FTIR spectrum for SOPC free in CH_2 stretching vibration are shown in (Fig 4.8), The FTIR spectra of free SOPC shown in (Fig 4.9) and The FTIR spectra of SOPC-dgitonin thin films with concentrations (0.1, 0.2, 0.3, 0.4, 0.5 and 0.6mM) are shown in (Fig 4.10) .

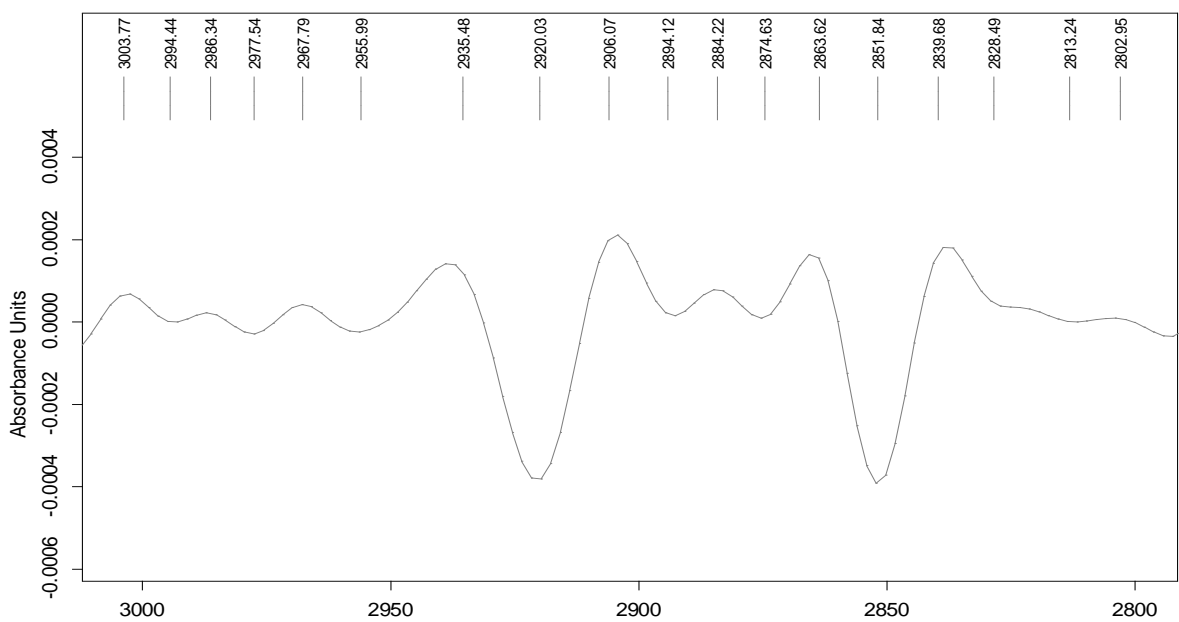


(Fig 4.9) :The second derivative of the FTIR spectrum for SOPC free in CH_2 stretching vibration.

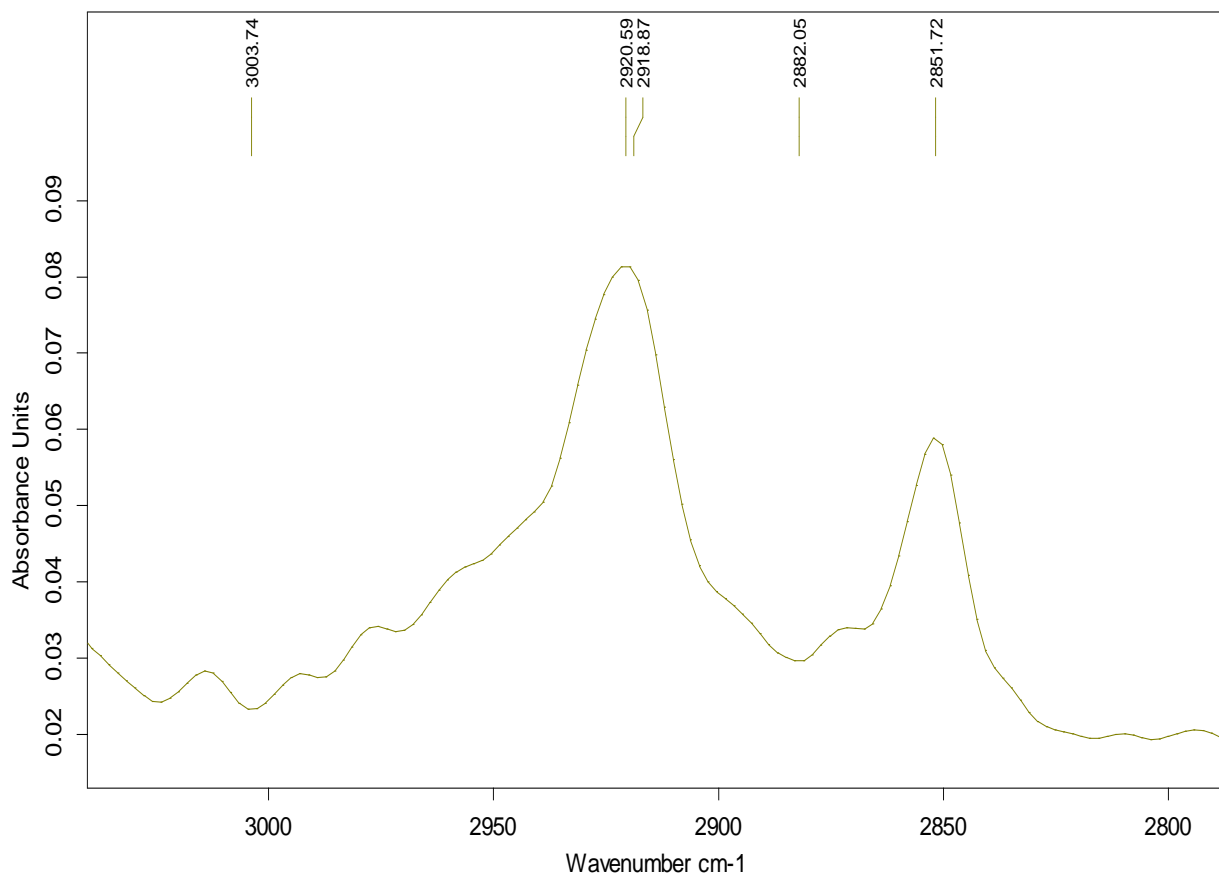


(Fig 4.10) :The FTIR spectra of free SOPC .

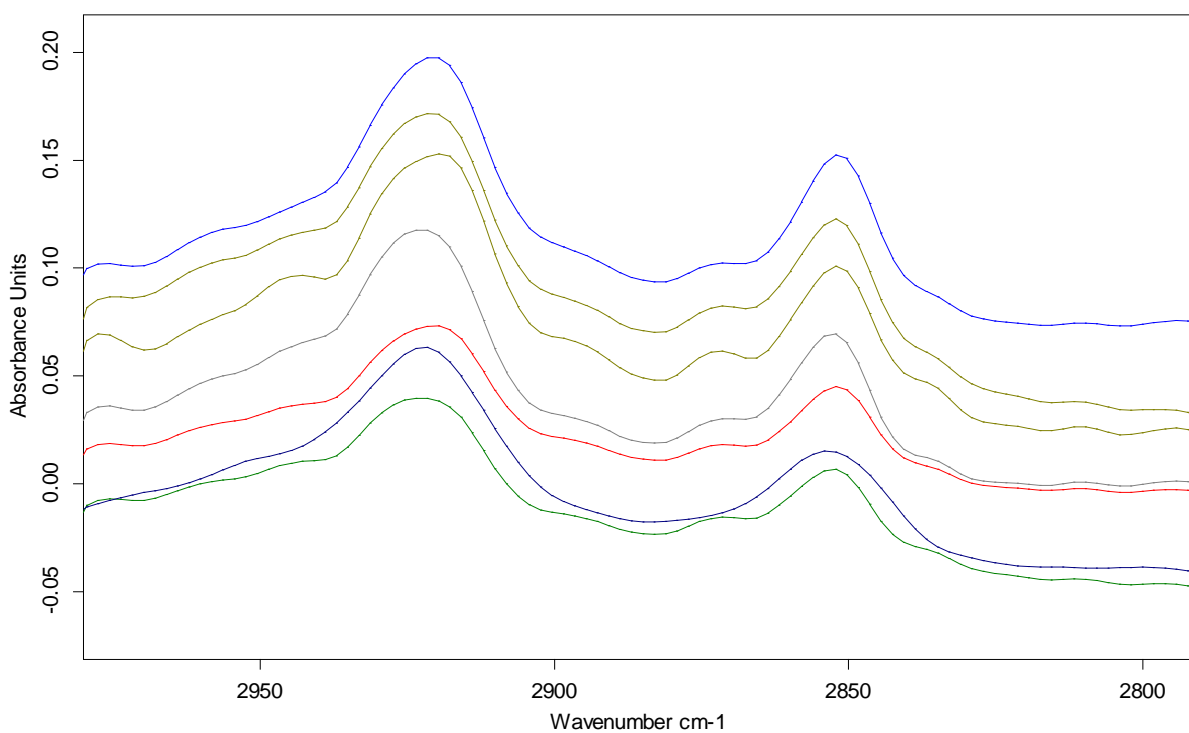


(Fig 4.11) : The FTIR spectra of SOPC-dgitonin thin films with concentrations (0.1, 0.2, 0.3, 0.4, 0.5 and 0.6mM) .

The peak positions of SOPC with different digitonin concentrations in CH₂ stretching are shown in (Table 4.1). For SOPC-digitonin spectrum we notice CH₃ stretching asymmetric ,CH₂ stretching asymmetric ,CH₃ stretching, symmetric ,and CH₂ stretching symmetric.

peak shifts in CH₂ stretching asymmetric: 2917 to 2915 cm⁻¹, CH₂ stretching symmetric :2851 to 2856 cm⁻¹ , CH₃ stretching asymmetric :2955 to 2957 cm⁻¹, CH₃ stretching symmetric : 2863 to 2869 cm⁻¹.

The vibrational energy is proportional to the frequency of oscillation. Shifts to higher wave numbers means that the frequency of oscillation has increased and so a photon of higher energy is needed to break the bond and it can be said that shifts toward higher wave numbers indicates an increase in the strength in the bond and vice versa.

The second derivative of the FTIR spectrum for SOPC free in C=O stretching and P-O₂⁻ stretching vibration are shown in (Fig 4.11),The FTIR spectra of free SOPC in C=O stretching and P-O₂⁻ stretching vibration shown in (Fig 4.12) and The FTIR spectra of SOPC-dgitonin in in C=O stretching and P-O₂⁻ stretching vibration thin films with concentrations (0.1, 0.2, 0.3, 0.4, 0.5and 0.6mM) are shown in (Fig 4.13) .

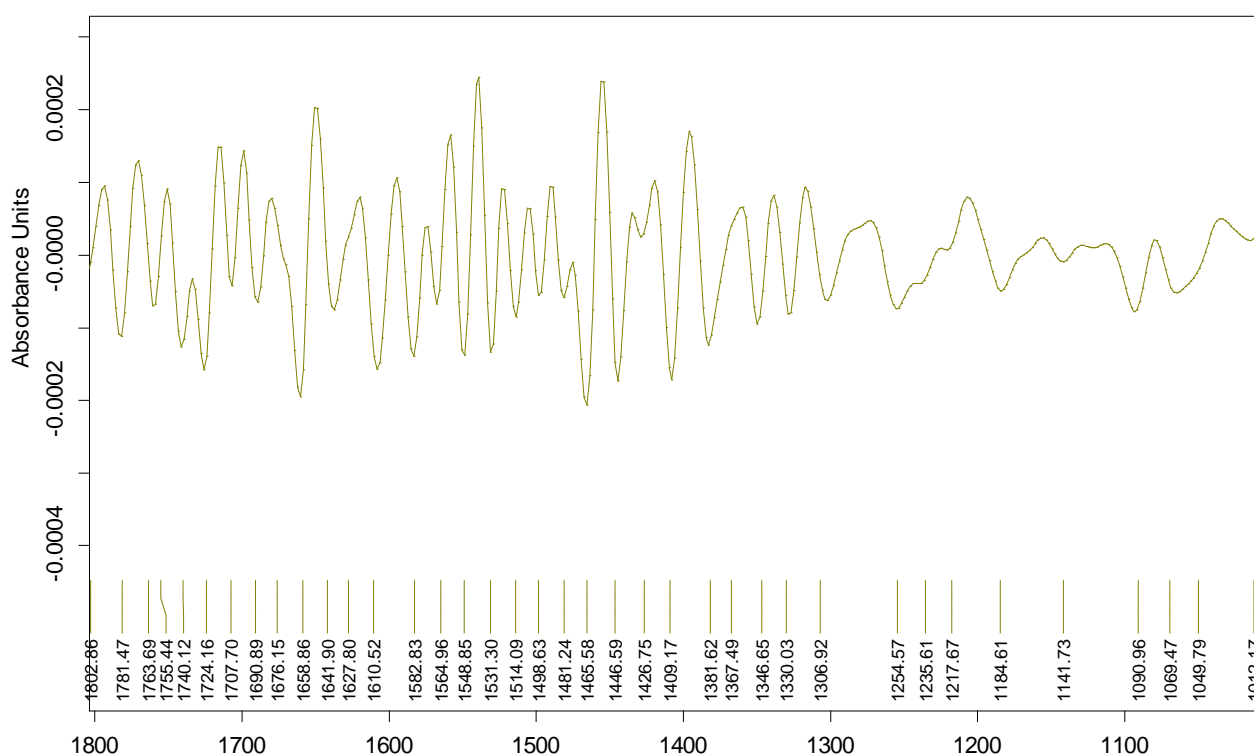


(Fig 4.12):The second derivative of the FTIR spectrum for SOPC free in C=O stretching and P-O₂⁻ stretching vibration .

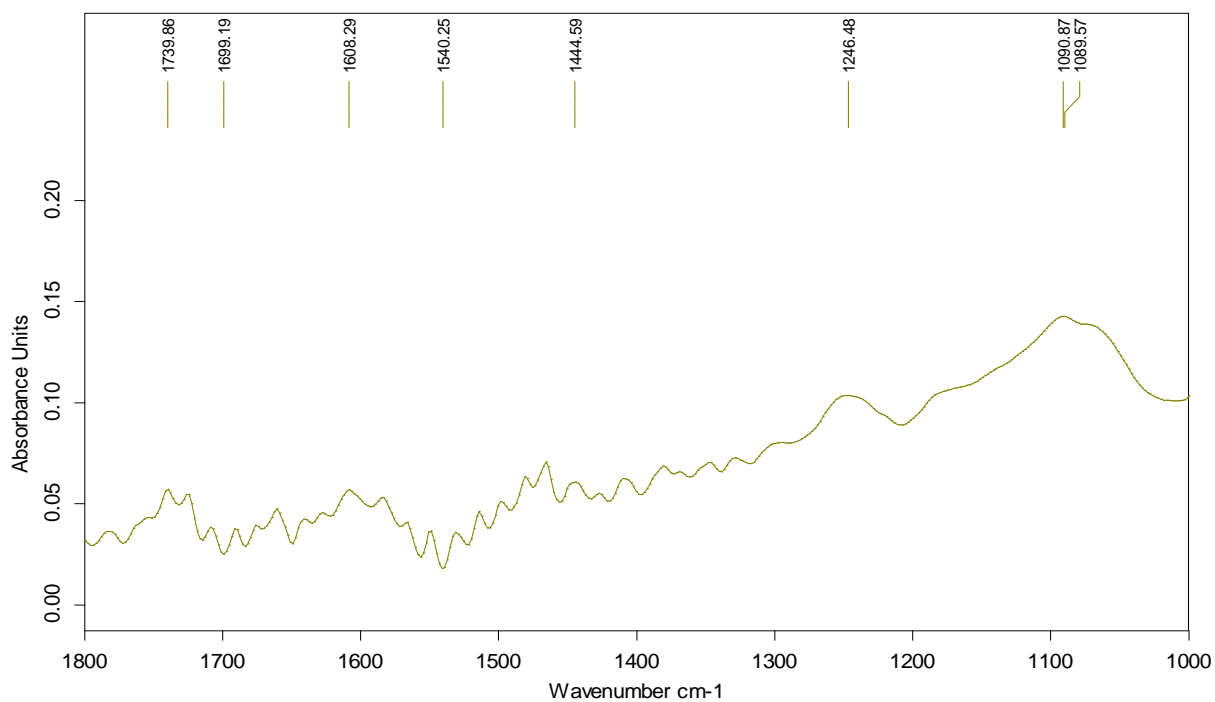


(Fig 4.13):The FTIR spectra of free SOPC in C=O stretching and P-O²⁻ stretching vibration.

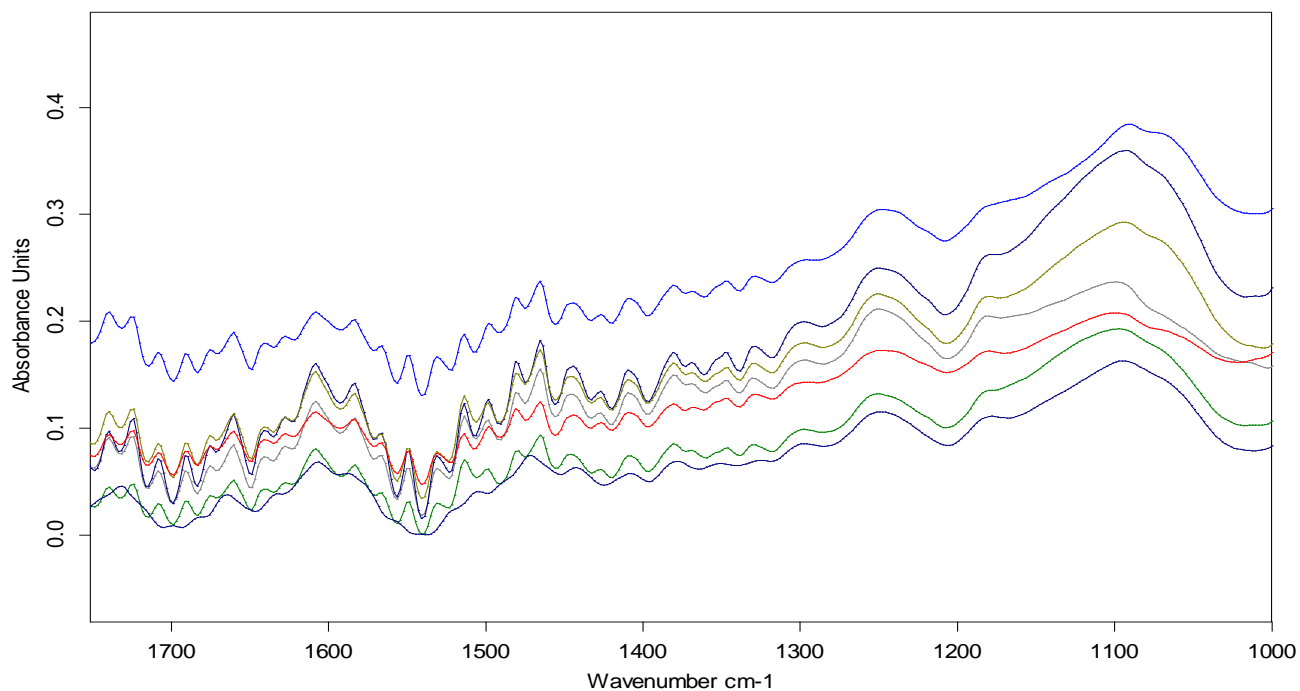


(Fig 4.14) :The FTIR spectra of SOPC-dgintonin in C=O stretching and P-O²⁻ stretching vibration thin films with concentrations (0.1, 0.2, 0.3, 0.4, 0.5 and 0.6mM) .

peak shifts in C=O stretching: 1724 to 1740 cm^{-1} , PO_2^- stretching, asymmetric :1217 to 1221 , PO_2^- stretching, symmetric: 1069 to 1080.

Table 4.2: Bands assignment in the absorbance spectra of SOPC with different digitonin concentrations .

Bands	SOPC free	SOPC-digitonin 0.1mM	SOPC-digitonin 0.2mM	SOPC-digitonin 0.3mM	SOPC-digitonin 0.4mM	SOPC-digitonin 0.5mM	SOPC-digitonin 0.6mM
Region I							
CH ₂ stretching asymmetric.	2917	2917	2916	2917	2916	2916	2915
CH ₂ stretching symmetric.	2851	2851	2852	2851	2855	2854	2856
CH ₃ stretching asymmetric.	2955	2957	2959	2954	2956	2958	2957
CH ₃ stretching symmetric.	2863	2861	2868	2862	2865	2865	2869
Region II							
C=O stretching	1724	1726	1725	1729	1738	1742	1740
Region III							
PO_2^- stretching, asymmetric .	1217	1219	1216	1222	1219	1219	1221
PO_2^- stretching, symmetric.	1079	1081	1079	1083	1076	1080	1080

In region I there is one strong positive feature at 2851 cm^{-1} in addition to a one weak positive feature at 2917 cm^{-1} . For region II there is one strong positive feature at 1724 cm^{-1} . These features were obtained at digitonin concentrations (0.4, 0.5, and 0.6 mM), for region III there is no strong positive feature at 1217 cm^{-1} in addition to another one weak positive feature at 1079 cm^{-1} .

It is clearly shown that the strong positive features in region I and region II become stronger as digitonin concentration was increased.

The observed positive features are attributed to the increase in the intensity of the region I at 2851 cm^{-1} , region II at 1738 cm^{-1} , and region III at $1217, 1079 \text{ cm}^{-1}$ as a result of SOPC interaction with digitonin .

Chapter Five

Conclusions and future work

Chapter five

5.1 Conclusions.

In this research, the Interactions between Digitonin and 1-Stearoyl-2-oleoyl-*sn*-glycero-3-phosphocholine (SOPC) has been studied using UV-vis spectroscopy, fluorescence spectroscopy, and FTIR spectroscopy. The binding parameters for the binding of digitonin with SOPC have been determined: For SOPC-digitonin the binding constants is calculated by UV-vis spectroscopy to be $K = 5.324 \times 10^3 M^{-1}$. The obtained values of the binding constants K by using fluorescence spectroscopy is $5.191 \times 10^3 M^{-1}$. Which agree with the values obtained by UV-vis spectroscopy. In addition, the values of Stern-Volmer quenching constant and quenching rate constant for SOPC-digitonin have been measured to be $[1.05 \times 10^3 Lmol^{-1}, 1.05 \times 10^{11} Lmol^{-1}s^{-1}]$.

These experimental results confirm the fact that dynamic quenching is not the main mechanism that causes the fluorescence quenching, and the decrease in fluorescence intensity occurred as a result of static quenching, which is indicative of a complex formation between the SOPC and digitonin. Also the low binding constant between the digitonin and SOPC is due to the effective hydrogen bonding .

Analysis of the FTIR spectra reveals that SOPC interaction has induced reduction in the absorption band of region I accompanied with an increase with different proportionality due to the different accessibility of H-bond formation in these components. This decrease in the intensity with increasing digitonin concentration . On the other hand, analysis of the FTIR spectra for SOPC interaction reveals that a decreasing in the intensity of the absorption band of regions II and III with increasing digitonin concentration has occurred .

5.2 Future work.

The binding study of Digitonin and 1-Stearoyl-2-oleoyl-*sn*-glycero-3 phosphocholine is of great importance in pharmacology and biochemistry. Our research can provide important information to medical and clinical researches .

References :

- Akiyama, T.; Takagi, S.; Sankawa, U.; Inari, S.; Saito, H. Saponin–Cholesterol Interaction in the Multibilayers of Egg Yolk Lecithin as Studied by Deuterium Nuclear Magnetic Resonance: Digitonin and Its Analogues. *Biochemistry* 1980, 19, 1904–1911.
- Ball, D.W. (2001). *The basics of spectroscopy*, SPIE- the international society for optical engineering.
- Banwell, C. N.(1972): *Fundamentals of Molecular Spectroscopy*. 2nd ed., McGRAW- HILL Bokk Company (UK) Limited.
- Casal, H.L., Mantsch, H.H., 1984. Polymorphic phase behavior of phospholipid membranes studied by infrared spectroscopy. *Biochim. Biophys. Acta* 779, 381–401.
- Cooper, A. (2004). *Biophysical Chemistry*, The Royal Society of Chemistry, UK.
- De Geyter, E.; Smagghe, G.; Rahbe, Y.; Geelen, D. Triterpene Saponins of Quillaja Saponaria Show Strong Aphicidal and Deterrent Activity against the Pea Aphid *Acyrtosiphon Pisum*. *Pest Manage. Sci.* 2012, 68, 164–169.
- Derrick, M.R., Stulik, D., Landry, J.M.. (1999): *Infrared Spectroscopy in Conservation Science*. The Getty Conservation Institue, Los Angelos.
- Dong, C.Y., So, P.T.. (2002). *Fluorescence Spectrophotometry*. Massachusetts Institute of Technology, macmillan Publishers Ltd.
- Fiskum, G.; Craig, S. W.; Decker, G. L.; Lehninger, A. L. The Cytoskeleton of Digitonin-Treated Rat Hepatocytes. *Proc. Natl. Acad. Sci. U.S.A.* 1980, 77, 3430–3434.
- Flower KR, Khalifa I, Bassan P, Demoulin D, Jackson E, Lockyer NP, McGown AT, Miles P, Vaccari L, Gardner P: Synchrotron FTIR analysis of drug treated ovarian A2780 cells: An ability to differentiate cell response to different drugs? *Analyst* 2011, 136(3):498-507.
- Fringeli, U.P., Gu'nthard, H.H., 1981. Infrared membrane spectroscopy. In: Grell, E. (Ed.), *Membrane Spectroscopy*. Springer, Berlin, pp. 270–332.
- Griffith, P.R., Haseth, J.A. (2007). *Fourier Transform Infrared Spectroscopy*, 2nd ed., John Wiley & sons. Inc.
- Gomez-Fernandez, J. C.; Corbalan-Garcia, S. Diacylglycerols, Multivalent Membrane Modulators. *Chem. Phys. Lipids* 2007, 148, 1-25.

- Hildebrandt, P., Siebert, F.(2008): *Vibrational Spectroscopy in Life Science*, 1st, John Wiley & Sons Ltd,UK.
- Hollas, M.J. (2004). *Modern spectroscopy*. 4th ed., John Wiley & sons, Chichester, England.
- Hostettmann, K.; Marston, A. *Chemistry and Pharmacology of Natural Products: Saponins*; Cambridge University Press: New York, 1995.
- Hannun, Y.A.; Obeid, L.M. Principles of Bioactive Lipid Signaling: Lessons from Sphingolipids. *Nature Reviews: Mol. Cell Bio.* **2008**, 9, 139–150.
- Johnson. L., Spence. T. Z. M.. (2010). *Fundamental of fluorescence.Molecular Probes Handbook, A Guide to Fluorescent Probes and Labeling Technologies*.11th ed.
- Keukens, E. A.; de Vrije, T.; Fabrie, C. H.; Demel, R. A.; Jongen, W. M.; de Kruijff, B. Dual Specificity of Sterol-Mediated Glycoalkaloid Induced Membrane Disruption. *Biochim. Biophys. Acta* 1992, 1110,127–136.
- Kong,J., Yu, Sh..(2007). Fourier Transform Infrared Spectroscopic Analysis of Protein Secondary Structures. *Acta biochimica et Biophysica Sinica*, 39(8), P 549-559.
- Krishan A: Rapid flow cytofluorometric analysis of mammalian cell cycle by propidium iodide staining. *Journal of Cell Biology* 1975, 66(1):188-193.
- Lakowicz, J. R. (2006): *Principles of Fluorescence Spectroscopy*, 3 rded, Springer Science+Business Media, LLC .
- Lakowicz, J. R. (2006): *Principles of Fluorescence Spectroscopy*, 3 rded, Springer Science+Business Media, LLC .
- Lee, D.C., Chapman, D., 1986. Infrared spectroscopic studies of biomembranes and model membranes. *Biosci. Rep.* 6,235–256.
- Li, Y., He, W.Y., Liu, H., Yao, X., Hu, Z. (2007). *Journal of Molecular Structure*, 831, P 144.
- Liu, J.; Xiao, N.; DeFranco, D. B. Use of Digitonin-Permeabilized Cells in Studies of Steroid Receptor Subnuclear Trafficking. *Methods Enzymol.* 1999, 19, 403–409.
- Luckey, D. *Membrane Structural Biology with Biochemical and Biophysical Foundations*, 1st ed.; Cambridge University Press: New York, 2008.

- Mantsch, H.H., McElhaney, R.N., 1991. Phospholipid phase transitions in model and biological membranes as studied by infrared spectroscopy. *Chem. Phys. Lipids* 57, 213–226.
- Murphy, E.; Coll, K.; Rich, T. L.; Williamson, J. R. Hormonal Effects on Calcium Homeostasis in Isolated Hepatocytes. *J. Biol. Chem.* 1980, 255, 6600–6608.
- Nelson, D. L. and Cox, M. M. *Lehninger Principles of Biochemistry*, 4th ed.; W.H. Freeman: New York, 2004.
- Pavis, D. et al. (2008). *Introduction to spectroscopy*. 4th ed., cengage learning.
- Pavia, D. L., Lampman, G. M., Kriz, G. S., Vyvyan, J. R (2009): *Introduction to Spectroscopy*, 4th, Brooks/Cole, Cengage learning, USA.
- Subodh Kumar. (2006): *Spectroscopy of Organic Compounds*.
- Schmidt, W. (2005). *Optical spectroscopy in chemistry and life sciences*. WILEY-VCMVerlag GmbH & Co, Weinheim, Germany.
- Schulman, S.G. (1977). *Fluorescence and phosphorescence spectroscopy: physiochemical principles and practice*, Vol 59, A. Wheaton & Co. Ltd, Exeter
- Settle, F.A (1997): *Handbook of Instrumental Techniques for Analytical Chemistry, Infrared Spectroscopy*, Prentice Hall PTR (ECS Professional).
- Sheehan, D. (2009). *Physical Biochemistry: principles and applications*. 2nd ed., John Wiley & sons Ltd.
- Shernan, M. (2014). *Infrared Spectroscopy: A Key to Organic Structure*, Yale-New Haven Teachers Institute.
- Soukpo'e-Kossi, C. N. N., Sedaghat-Herati, R., Hotchandani, S., Tajmir-Riahi, H.A. (2007). *International Journal of Biological Macromolecules*, 40, p 484–490.
- Stearns, M. E.; Ochs, R. L. A. 1982 Functional In Vitro Model for Studies of Intracellular Motility in Digitonin-Permeabilized Erythrocytes. *J. Cell Biol.* 1982, 94, 727–739.
- Stuart, B. (2004). *Infrared spectroscopy: Fundamentals and applications*. John Wiley & Sons, Ltd, Kent, UK.
- Takai, Y. K.; Kikkawa, A.; Mori, U.; Nishizuka, Y. 1979 Unsaturated Diacylglycerol as a Possible Messenger for the Activation of Calcium-Activated, Phospholipid-Dependent Protein Kinase System. *Biochem. Biophys. Res Commun.* 1979, 91, 1218-1224.

- Thakur, M.; Melzig, M. F.; Fuchs, H.; Weng, A. 2011 Chemistry and Pharmacology of Saponins: Special Focus on Cytotoxic Properties. *Botanics: Targets Therapy* 2011, 1 –29.
- Thermo Nicolet (2001). *Introduction to Fourier Transform Infrared Spectrometry*, Thermo Nicolet Corporation, USA.
- Turro, N.J. (1991). *Modern Molecular Photochemistry*, University science books, America.
- Uversky, V.N., Permykov, A.E. (2007): *Methods in Protein Structure and Stability Analysis; Vibrational spectroscopy*, Nova Science Publishers, Inc, Hauppauge, New York.
- Vij, D. R. (2006): *Handbook of Applied Solid State Spectroscopy*, Springer Science+Business Media, LLC, USA.
- Williams, D. (1976), *methods of experimental physics: spectroscopy*, vol 13, part A, Academic press Inc.
- Wilson, R.A., and Bullen, H.A. *Introduction to Scanning Probe Microscopy (SPM):Basic Theory Atomic Force Microscopy (AFM)*. Department of Chemistry, Northern Kentucky University, Highland Heights, KY 41099.
- Wink, M.; van Wyk, B.-E. *Mind-Altering and Poisonous Plants of the World*; Timber Press: London, 2008.
- Workman, J. R. (1998): *Applied Spectroscopy: Optical Spectrometers*, Academic Press, San Diego.
- Yadav, L.D. (2005). *Organic spectroscopy*, Klower academic publisher, New Delhi, India.
- Yu, B.; Choi, H. The Effects of Digitonin and Glycyrrhizin on Liposomes. *Arch. Pharmacol Res.* 1986, 9, 119–125.
- Zuurendonk, P. F.; Tager, J. M. Rapid Separation of Particulate Components and Soluble Cytoplasm of Isolated Rat-Liver Cells. *Biochim. Biophys. Acta* 1974, 333, 393–399.

دراسة تأثير الديجوتنين على احد انواع الدهون المكونة للخلية (SOPC) بواسطة تقنيات مطيافية الجزيئات.

اسم الطالب : ابراهيم غازي موسى هوارين .

اسم المشرف : الدكتور .موسى ابو طير و الدكتور .حسن دويك.

ملخص

ديجيتونين هو سابونين الستيرويد الستيرويدي، وهي فئة من المنتجات الطبيعية التي يمكن أن ترتبط بالكوليسترول و سطح الخلايا . على الرغم من معرفة نشاط تحليل غشاء الخلية، فإنه لا يزال من غير الواضح كيف يتفاعل مع أغشية الخلايا . في هذا العمل، تم التحقيق الكمي لآلية التفاعل بين الديجيتونين و (1-ستيرويد-2-أوليويول-سن-جليسيرو-3-فوسفهوسولين).

تم دراسة التفاعل بين الديجيتونين و احد انواع الدهون المكونة للغشاء للخلية (SOPC) باستخدام مطياف الأشعة فوق البنفسجية (Fluorescence spectrophotometer) و جهاز انبعاث الأشعة (UV-vis spectrophotometer) و جهاز مطياف تحويل فوريير للأشعة تحت الحمراء (Fourier transform infrared spectroscopy) في هذه التجربة تم حساب ثابت الترابط (binding constant) للفوسفوليبيد و الديجيتونين عن طريق جهاز مطياف الأشعة فوق البنفسجية و القيمة هي $5.324 \times 10^3 M^{-1}$ اما تحليل طيف الانبعاث اوصل الى حساب ثابت الترابط للتفاعل $5.191 \times 10^3 M^{-1}$ مما يشير الى نتائج متقاربة لثابت الترابط عن طريق طرق الحساب المختلفة .

تم حساب ثابت (Stern-Volmer constant) و ثابت (quenching rate) للترابط بين الديجيتونين و الفوسفوليبيد وهي $1.05 \times 10^3 l mol^{-1}$, $1.05 \times 10^{11} l mol^{-1}$ على التوالي

في هذا الاختبار من الجسيمات الكبيرة من (SOPC) و تراكيز مختلفة من الديجيتونين تم تحديد كيفية تفاعل الديجيتونين مع (SOPC)، و النتائج التي تم التوصل اليها ان شدة امتصاص الأشعة فوق البنفسجية للفوسفوليبيد تقل كلما زاد تركيز الديجيتونين و هذا ما تبين في حالة استخدام جهاز انبعاث الأشعة و جهاز مطياف تحويل فوريير للأشعة تحت الحمراء .